Abstract

Liquid phase hydrogenation of 1-hexene under mild conditions has been investigated on a series of silica (SiO_2 and MCM-41) supported Pd catalysts prepared from different Pd precursors such as $Pd(NO_3)_2$, $PdCl_2$, and $Pd(OOCCH_3)_2$. For any silica support, use of $PdCl_2$ as a precursor resulted in smaller Pd particles, higher dispersion, and consequently higher hydrogenation activities. Supported Pd catalysts prepared from $PdCl_2$ showed greater metal sintering after 5-h batch reaction. However, leaching of Pd was found to occur to a significant degree for the catalysts prepared from $Pd(NO_3)_2$ and $Pd(OOCCH_3)_2$. The results suggest that deactivation of the silica-supported Pd catalysts in liquid phase hydrogenation is dependent on the palladium particle size with smaller Pd particles being more susceptible to sintering while larger particles are more likely to be leached. An optimum Pd particle size may be needed in order to minimize such loss and enhance Pd dispersion.

1. Introduction

Silica-supported Pd catalysts are commercially attractive for liquid-phase catalytic hydrogenation in many organic syntheses [1-6]. The major advantages of supported noble metal catalysts are their relatively high activity, mild process conditions, easy separation, and better handling properties. Since the catalytically active phase for hydrogenation is the metallic phase, having palladium well-dispersed and reduced is required for a catalyst to have high activity. Different preparation techniques have been tried in order to obtain catalysts with small metal particles and high metal dispersions. Recently, it has been reported that silica-supported Pd nanoparticles prepared by reduction of an organometallic precursor palladium(II) bis-dibencylidene with H_2 showed remarkable liquid-phase hydrogenation activity of different organic substrates [2]. However, an increase in particle size was observed after the fourth batch of 1-hexene hydrogenation at 25^{o}C.

Sintering of supported metal particles is typically irreversible and can occur even at ambient temperature because of atomic migration processes involving the extraction and transport of surface metal atoms by chelating molecules [7]. Despite a high number of factors potentially involved in catalyst deactivation in liquid phase organic reactions (sintering or leaching of active components, poisoning of active sites by heteroatom-containing molecules, inactive metal or metal oxide deposition, impurities in solvents and reagents, oligomeric or polymeric by-products), the mechanisms for such deactivation have not been studied very often. For example, the effects of metal dispersion and support texture and porosity on the activity and the deactivation of supported Pd catalysts in liquid phase hydrogenation remain unclear.

In this study, we investigated the activities and deactivation of Pd/MCM-41 and Pd/SiO_2 catalysts prepared with different Pd precursors [$Pd(NO_3)_2$, $Pd(OOCCH_3)_2$, and $PdCl_2$] for liquid phase hydrogenation of 1-hexene under mild conditions. In order to distinguish the effects of silica support structure from the effects of BET surface area and pore size, the SiO_2 and MCM-41 used as catalyst supports in this study possessed similar BET surface areas and narrow pore size distributions with average pore diameters of ca. 3 nm, albeit in slightly different forms of silica. The effects of Pd precursors and silica support structure were investigated in terms of metal dispersion, catalytic activity, and deactivation due to metal sintering and metal leaching.

2. Experimental

2.1 Preparation of Silica-Supported Pd Catalysts

The two types of silica supports used in this study were pure silica MCM-41 (S_{BET} = 921 m^2/g, r_p = 28 Å, V_p = 0.87 cc/g) and high surface area chromatographic grade SiO_2 (S_{BET} = 716 m^2/g, r_p = 22 Å, V_p = 0.39 cc/g). MCM-41 was prepared in the manner described by Cho et al. [8] using the gel composition of CTAB: $0.3NH_3$: $4SiO_2$: Na_2O: $200H_2O$, where CTAB denotes cetyltrimethyl ammonium bromide. High surface area SiO_2 was obtained commercially from Grace Davison Co., Ltd. The catalysts were prepared by impregnation using a slight excess of the amount of solution of different palladium precursors [$Pd(NO_3)_2$, $PdCl_2$, or $Pd(OOCCH_3)_2$ (Aldrich)] required to fill the pore volume of the supports. The catalysts were dried overnight at 110°C and then calcined in air at 500°C for 2 h. The final Pd loadings of the calcined catalysts were determined using atomic absorption spectroscopy (Varian Spectra A800) to be approximately 0.5 wt% palladium content.

2.2 Catalyst Characterization

XRD of the catalysts was carried out from 20-80° 2θ using a SIEMENS D5000 X-ray diffractometer and Cu K_α radiation with a Ni filter. Relative percentages of palladium dispersion were determined by pulsing carbon monoxide over the reduced catalyst. Approximately 0.2 g of catalyst was placed in a quartz tube in a temperature-controlled oven. CO adsorption was determined by a thermal conductivity detector (TCD) at the exit. Prior to chemisorption, the catalyst was reduced in a flow of hydrogen (50 cc/min) at room temperature for 2 h. Then the sample was purged at this temperature with helium for 1 h. Carbon monoxide was pulsed at room temperature over the reduced catalyst until the TCD signal from each successive pulse was constant. The TPR profiles of supported palladium catalysts were obtained by temperature-programmed reduction using an in-house system and a temperature ramp of 5°C/min from 30 to 300°C in a flow of 5% H_2 in argon. Approximately 0.20 g of a calcined catalyst was placed in a quartz tube in a temperature-controlled oven and connected to a thermal conductivity detector (TCD). The H_2 consumption was measured by analyzing the effluent gas with a thermal conductivity detector.

2.3 Liquid-Phase Hydrogenation

Liquid-phase hydrogenation reactions were carried out at 25°C and 1 atm in a 100 ml stainless steel Taiatsu autoclave. Approximately 0.1 gram of supported Pd catalyst was placed into the autoclave. The system was purged with nitrogen to remove the remaining air. The supported Pd catalyst was reduced *in-situ* with hydrogen at room temperature for 2 h. The reaction mixture composed of 1 ml of 1-hexene and 7 ml ethanol was first kept in a 100 ml feed column. The reaction mixture was introduced into the reactor with nitrogen to start the reaction. The amount of hydrogen consumption was monitored every five minutes by noting the change in pressure of the hydrogen. The stirring rate used in this study was 800 rpm, sufficient to ensure that the reaction rate did not depend on the stirring rate (as determined). The liquid reactants, products, and the head space gases were analyzed by gas chromatography using a Shimazu GC-9A equipped with a FID detector. No reduction or decomposition of ethanol during the reaction was observed.

3. Results and Discussion

3.1 Characteristics and catalytic behavior for 1-hexene hydrogenation

The characteristics of the catalysts based on CO chemisorption, XRD, and TEM results and their catalytic activities for 1-hexene hydrogenation are reported in Table 1. A suitable temperature for calcination of all palladium precursors was determined by thermogravimetric analysis of bulk palladium nitrate, palladium acetate, and palladium chloride (not shown). All palladium precursors appeared to be fully decomposed for calcination temperatures above 400^{o}C. Thus, a calcination procedure using 500^{o}C for 2 hours was used. The presence of the palladium oxide phase (PdO) after calcination prior to reduction was confirmed by XRD results for all but the most highly dispersed catalysts prepared from $PdCl_2$ (Figure 1). The major diffraction peak for PdO was detectable at 33.8^{o} 2θ for the catalysts prepared from $Pd(NO_3)_2$ and $Pd(OAc)_2$. The average PdO crystallite sizes were calculated using the Scherrer's equation [9] with the catalysts prepared from $Pd(OAc)_2$ showed the largest PdO particle size. Supported Pd catalysts prepared from $PdCl_2$ did not exhibit any distinct XRD patterns. This suggests that the crystallite sizes of PdO prepared from $PdCl_2$ were below the lower limit for XRD detectability (3-5 nm). TEM analyses (Figure 2) gave results in good agreement with the crystallite size inferred from XRD. The differences in PdO particle sizes on different supports can also be ascribed to differences induced by both the support and the Pd precursor on sintering of palladium during preparation.

Temperature programmed reduction is a powerful tool to investigate the reducibility of the catalyst as a function of temperature. TPR profiles of all the catalyst samples are shown in Figure 3. It was found that the catalysts reduced readily to PdH_2 once hydrogen was introduced to the system, which is typical for supported Pd catalysts [10]. For the MCM-41 supported catalysts, a small reduction peak at ca. 65^{o}C was observed for all the catalysts prepared with different Pd precursors. This peak has been attributed to a portion of the PdO that could not be reduced at ambient temperature [11-12]. It should, however, be noted that the reduction of the catalysts measured after 2 h hydrogen flow maybe different from that under 5%H_2/Ar in the TPR conditions. Temperature programmed study (TPO) revealed that a minimal amount (< 10%) of PdO was not reduced at room temperature after 2 h exposure to hydrogen (results not shown). A significant negative peak at ca. 85^{o}C was observed for all the catalysts, this peak can be attributed to the decomposition of PdH_2 [13].

Although the MCM-41 possessed higher BET surface area and pore volume than the SiO_2, the catalysts prepared on both supports showed similar Pd dispersions and hydrogenation activities. For a given type of silica support, the activities of the catalysts were found to be in the order: Pd-Cl >> Pd-NO_3 ≈ Pd-Ac. The turnover frequencies were calculated using the number of surface metal atoms measured by CO-chemisorption. Since the TOFs were not significantly different for any of the catalysts, the internal resistance due to diffusion within the pores of the reactant species probably did not have any influence on the catalytic activity of the catalysts. The overall catalyst activities were, thus, merely dependent on the Pd dispersion based on CO chemisorption results (as seen by the similar TOFs).

The effects of Pd precursors on the catalyst activity in hydrogenation reactions have been reported by many groups [10, 14-18]. Pd catalysts supported on CeO_2 [14], SiO_2 or Al_2O_3 [15] prepared from $PdCl_2$ showed higher activities than those prepared from $Pd(NO_3)_2$ for CO hydrogenation. Mahata and Vishwanathan [16] reported that $Pd(OOCCH_3)_2$ offered better dispersion of Pd on alumina than $PdCl_2$ or $Pd(NH_3)_4Cl_2$. Phenol

hydrogenation activity over these catalysts was found to be a direct function of available palladium surface area. Recently, in a study of the catalytic reduction of NO to N_2 over supported Pd catalysts, Pd catalysts supported on EDTA-activated γ-Al_2O_3 prepared from $Pd(NO_3)_2$ were found to exhibit higher activities than those prepared from $PdCl_2$ [18]. The contradiction of the influence of palladium precursors on activities of supported Pd catalysts in the literature suggests that, besides Pd metal particle size and Pd dispersion, the precursor- or the metal-support interaction may also play an important role in determining the catalytic properties of the catalysts.

It should be noted that, when chloride-containing compounds were used as the catalyst precursor, the presence of residual chloride has been found occasionally in supported metal catalysts [19-20] and then the catalyst activity has decreased. However, in this work the catalysts prepared from $PdCl_2$ were found to exhibit higher hydrogenation activities than the ones prepared from $Pd(NO_3)_2$ or $Pd(OOCCH_3)_2$; thus we conclude that there was probably no residual chloride blocking the palladium sites. Most of the residual chloride can be significantly removed during the reduction procedure, especially when water vapor is produced.

3.2 Catalyst deactivation during liquid phase hydrogenation

After 5-h of batch reaction, the catalysts were collected by simple filtration. Catalyst deactivation processes by metal sintering and by metal leaching were investigated. The results are reported in Table 2. From the CO chemisorption results, it was found that the active Pd surface of the spent catalysts decreased by half of those of the fresh catalysts. It was found that the catalysts prepared from $PdCl_2$ and having small PdO particles exhibited greater Pd sintering. The particle sizes of Pd-Cl catalysts increased by 100-124% (from 4.8-5.1 nm to 9.6-11.4 nm), while those of Pd-NO_3 and Pd-Ac were not significantly changed. We wanted to avoid the influence of carbon deposits on the pore structure and on the contrast of the TEM images; after being taken out from the reactor and dried at room temperature, the catalysts were thus re-calcined in air at 500^{o}C for 2 h to remove any carbon deposits before characterization. The TEM micrographs of Pd-Cl/SiO_2 and Pd-Cl/MCM-41 catalysts after reaction and re-calcination are shown in Figure 4, larger PdO particle sizes were evident. The sintering probability can be higher when a metal particle is located closer to other particles. It is known that temperature, atmosphere, metal type and metal dispersion, promoters/impurities, and support surface area, texture and porosity are the principal parameters affecting rates of sintering [21]. However, the mechanism of metal sintering in liquid phase reactions has not been well investigated so far. Arai et al. have proposed that sintering occurs through transport of Pd metal between support and solvent as well as through transport on the support during Heck coupling reactions [22].

The percentages of palladium before and after 5-h of batch reaction were determined by atomic absorption spectroscopy. Palladium leaching occurred to a significant degree (30-40%) for the catalysts prepared from palladium nitrate and palladium acetate, whereas for the catalysts prepared from palladium chloride almost no Pd leaching was found. Pd leaching was little affected by the silica support structure (SiO_2 and MCM-41). The mechanism of metal leaching usually involves metal compounds that are formed and are soluble in the reaction mixture. Since it is unlikely that 1-hexene forms a compound with Pd at room temperature, unless it is some hydrido-organic complex, it is likely that Pd hydride formation is the cause of metal loss. It is well known that Pd particles are able to absorb hydrogen within their structure to form a Pd-β-

hydride phase. A number of publications [23-24] have reported that the formation of Pd hydride depends on the particle size of palladium; larger Pd particles more easily form Pd hydride, whereas smaller Pd particles may be unable to form the Pd-β-hydride phase. Under certain conditions, the Pd-β-hydride phase can appear as a soft material with higher mechanical abrasion [25]. This may be one reason why larger Pd particles form a Pd-β-hydride phase that is lost (leached) from the catalysts. The results were found to be in agreement with the previous work reported by our group that large Pd particles on silica supports result in Pd being leached during liquid phase hydrogenation reaction [12,26]. Recently, Mastalir et al. [27] showed that the Pd-β-hydride phase is catalytically inactive for hydrogenation reactions. Keeping palladium crystallites in a well-reduced, metallic state has also been suggested in order to prevent formation of soluble complex compounds during liquid phase hydrogenation reactions [28]. The results of this study emphasize the need for an optimum Pd particle size to maximize the surface area of Pd while minimizing metal deactivation by sintering and leaching.

4. Conclusions

In this research, we have studied the activity and deactivation of Pd/SiO_2 and Pd/MCM-41 catalysts prepared with different Pd precursors in liquid phase hydrogenation under mild conditions. Pd/MCM-41 showed similar Pd dispersion and catalytic activities for liquid phase hydrogenation of 1-hexene as Pd/SiO_2. Use of $PdCl_2$ as the Pd precursor for catalyst preparation resulted in smaller Pd particle sizes, greater Pd surface area, and, hence, higher hydrogenation activities. However, catalysts with smaller Pd particles (from $PdCl_2$) were found to exhibit also greater metal sintering during liquid phase reaction. Significant Pd leaching occurred for those catalysts with larger particles [prepared from $Pd(NO_3)_2$ and $Pd(OOCCH_3)_2$] due probably to formation of palladium hydride, which is known to form more easily on large Pd particles.

Acknowledgements

The financial supports of the Thailand Japan Technology Transfer Project (TJTTP-JBIC) and the Thailand Research Fund are gratefully acknowledged. The authors also would like to thank Professor Abdelhamid Sayari, University of Ottawa, Canada, and Dr. Aticha Chaisuwan, Chulalongkorn University, Thailand, for the assistance with MCM-41 preparation.

Table 1 Characteristics and catalytic activities for liquid phase hydrogenation of 1-hexene

Catalyst	CO uptake[a] (molecule $COx10^{18}$/g cat.)	% Pd dispersion	Pd^0 particle size[b] (nm)	PdO particle size (nm)		Rate constant $x10^3$ (mol/min/g cat.)	TOF[d] (s^{-1})
				XRD	TEM		
Pd-Ac/SiO_2	4.1	22.0	5.1	12.0	11.5	5.0	12.1
Pd-NO_3/SiO_2	4.0	17.7	6.3	10.0	10.1	4.0	10.0
Pd-Cl/SiO_2	8.4	26.1	4.3	n.d.[c]	4.8	8.5	10.2
Pd-Ac/MCM-41	4.1	17.7	6.3	13.0	12.0	4.1	10.0
Pd-NO_3/MCM-41	3.5	18.2	6.2	11.2	10.2	4.0	11.5
Pd-Cl/MCM-41	8.0	30.2	3.7	n.d.	5.1	8.3	10.4

[a]Error of measurement = +/- 5 %.

[b]Based on $d = 1.12/D$ (nm), where D = fractional metal dispersion [16].

[c]n.d. = not detected.

[d]Based on CO chemisorption results.

Table 2 Deactivation of various supported Pd catalysts during liquid phase hydrogenation of 1-hexene[a]

Catalysts	**CO chemisorption of the spent catalysts (molecule CO x 10^{18}/ g cat.)**	**%Increase of PdO particle size[b]**	**%Pd loss[c]**
Pd-Ac/SiO_2	2.5	7.8	36.4
Pd-NO_3/SiO_2	2.5	18.8	40.9
Pd-Cl/SiO_2	5.4	100	1.8
Pd-Ac/MCM-41	2.7	9.2	34.1
Pd-NO_3/MCM-41	1.7	24.5	41.2
Pd-Cl/MCM-41	3.8	123.5	2.1

[a]After 5-h batch hydrogenation reaction of 1-hexene at 25^{o}C and 1 atm.

[b]Based on XRD results.

[c]Determined from atomic absorption spectroscopy. Error of measurement = +/- 10%.

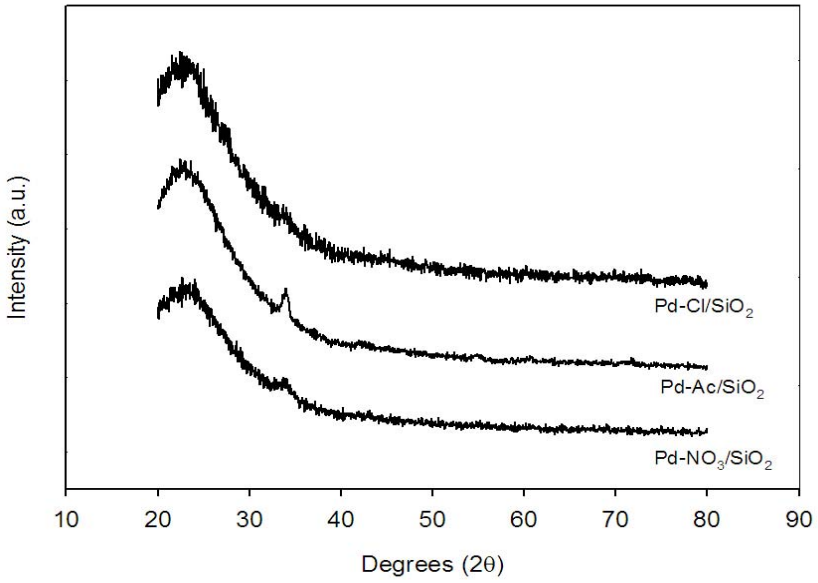

(a)

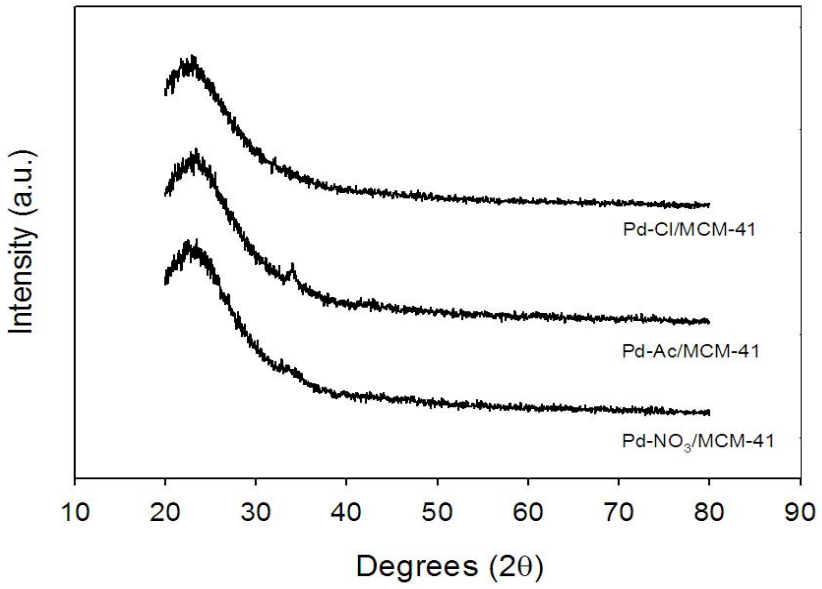

(b)

Figure 1 XRD patterns of various supported Pd catalysts prepared from different Pd precursors: (a) SiO_2-supported Pd catalysts, (b) MCM-41-supported Pd catalysts (after calcinations at 500^oC for 2 h).

50 nm

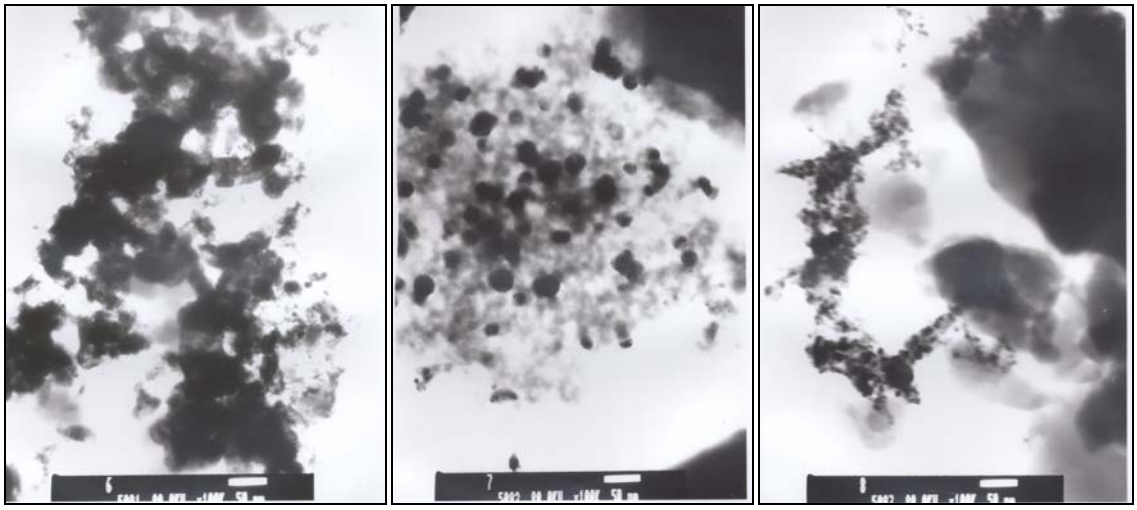

Pd-Ac/SiO_2 Pd-NO_3/SiO_2 Pd-Cl/SiO_2

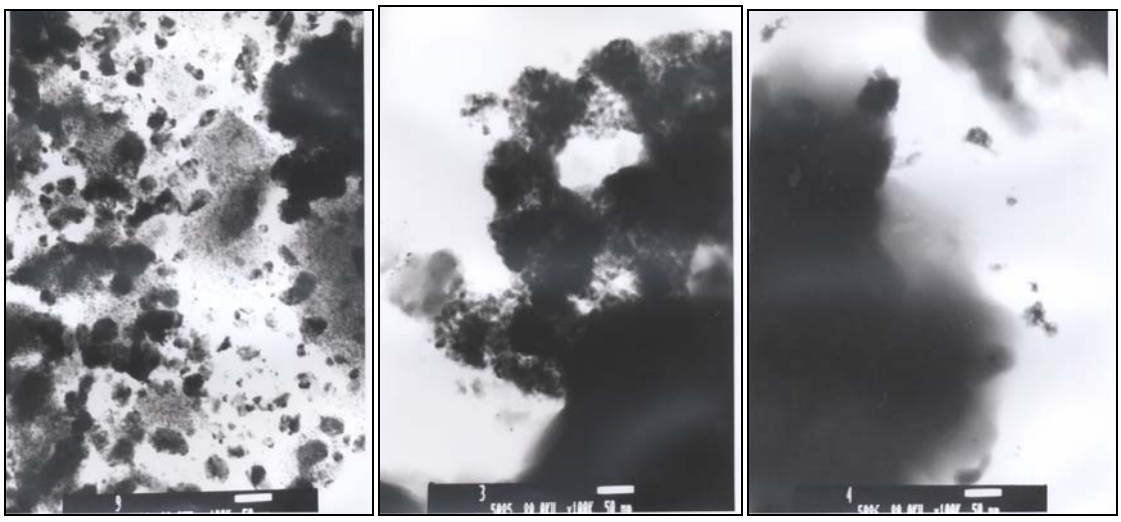

Pd-Ac/MCM-41 Pd-NO_3/MCM-41 Pd-Cl/MCM-41

Figure 2 TEM images of various supported Pd catalysts (after calcinations at 500^{o}C for 2 h).

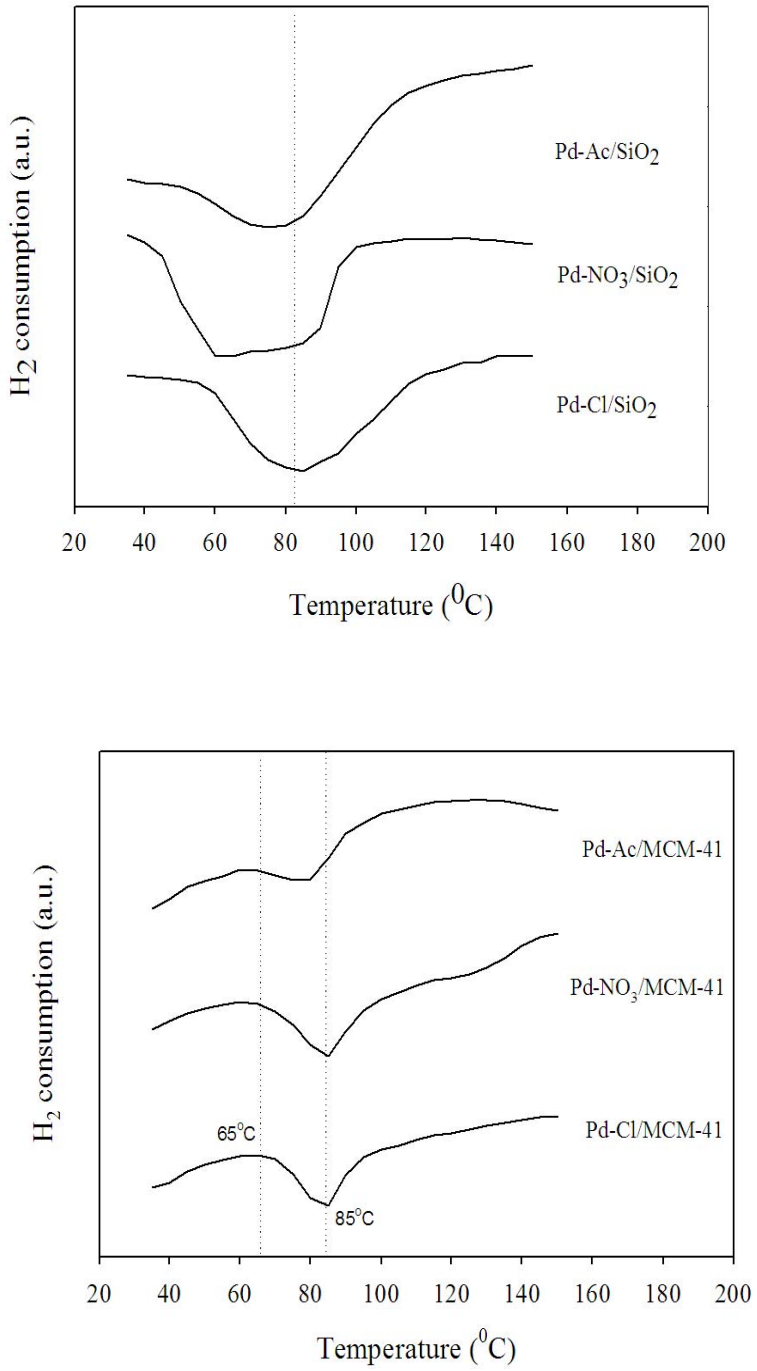

Figure 3 TPR profiles of various SiO_2 and MCM-41-supported Pd catalysts (after calcinations at 500°C for 2 h).

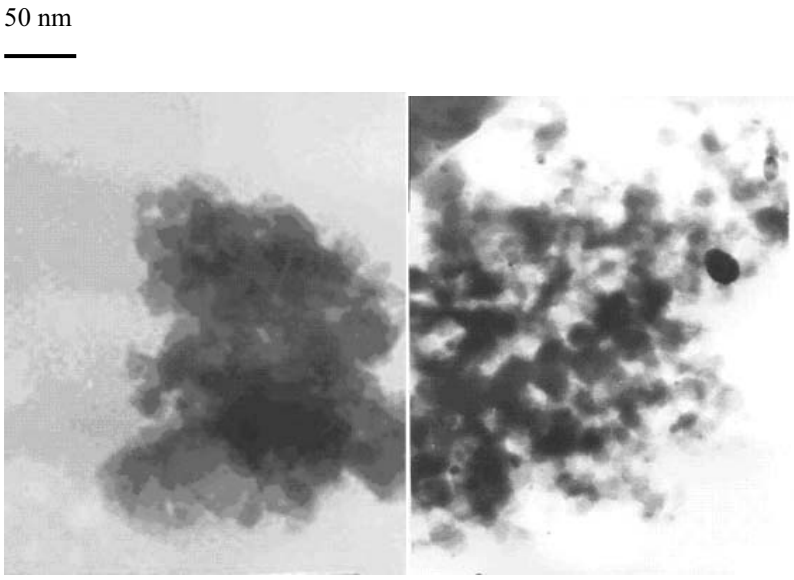

Figure 4 TEM micrographs of the (a) Pd-Cl/SiO_2 and (b) Pd-Cl/MCM-41 catalysts after reaction and re-calcination.

References

[1] L. Guczi, A. Horvath, A. Beck, A. Sarkany, Stud. Surf. Sci. Catal. 145 (2003) 351.

[2] O. Dominguez-Quintero, S. Martinez, Y. Henriquez, L. D'Ornelas, H. Krentzien, J. Osuna, J. Mol. Catal. A 197 (2003) 185.

[3] K. J. Stanger, Y. Tang, J. Anderegg, R. J. Angelici, J. Mol. Catal. A. 202 (2003) 147.

[4] I. Palinko, Appl. Catal. A 126 (1995) 39.

[5] T. Lopez, M. Asomoza, P. Bosch, E. Garcia-Figueroa, R. Gomez, J. Catal. 138 (1992) 463.

[6] T. A. Nijhuis, G. van Koten, J. A. Moulijn, Appl. Catal. A 238 (2003) 259.

[7] M. Besson, P. Gallezot, Catal. Today 81 (2003) 547.

[8] D. H. Cho, T. S. Chang, S. K. Ryu, Y. K. Lee, Catal. Lett. 64 (2000) 227.

[9] H. P. Klug, L. E. Alexander, X-ray diffraction procedures for polycrystalline

amorphous materials, 2nd ed., Wiley, New York, 1974.

[10] W. J. Shen, Y. Ichihashi , H. Ando, M. Okumura, M. Haruta, Y. Matsumura, Appl. Catal. A 217 (2001) 165.

[11] C. A. Koh, R. Nooney, S. Tahir, Catal. Lett. 47 (1997) 199.

[12] J. Panpranot, K. Pattamakomsan, P. Praserthdam, J. G. Goodwin, Jr., Ind. Eng. Chem. Res. 43 (2004) 6014.

[13] M. L. Cubeiro, J. L. G. Fierro, Appl. Catal. A 168 (1998) 307.

[14] W. J. Shen, Y. Ichihashi, M. Okumura, Y. Matsumura, Catal. Lett. 64 (2000) 23.

[15] S. H. Ali, J. G. Goodwin, Jr., J. Catal. 176 (1998) 3.

[16] N. Mahata, V. Vishwanathan, J. Catal. 196 (2000) 262.

[17] A. Gotti, R. Prins, J. Catal. 175 (1998) 302.

[18] D. Nazimek, W. Cwikla-Bundyra, Catal. Today 90 (2004) 39.

[19] Y. Zhou, M. C. Wood, N. Winograd, J. Catal. 146 (1994) 82.

[20] P. Johnston, R. W. Joyner, J. Chem. Soc. Faraday Trans. 89 (1993) 863.

[21] R. J. Farrauto, C. H. Bartholomew, Fundamentals of Industrial Catalytic Processes, Blackie Academic & Professional, London, 1997

[22] F. Zhao, K. Murakami, M. Shirai, M. Arai, J. Catal. 194 (2000) 479.

[23] W. J. Shen, M. Okumura, Y. Matsumura, M. Haruta, , Appl. Catal. A 213 (2001) 225.

[24] G. Neri, M. G. Musolino, C. Milone, D. Pietropaolo, S. Glavagno, Appl. Catal. A 208 (2001) 307.

[25] P. Albers, J. Pietsch, S. F. Parker, J. Mol. Catal. A 173 (2001) 275.

[26] J. Panpranot, K. Pattamakomsan, J. G. Goodwin, Jr., P. Praserthdam, Catal. Commun. 5

(2004) 583.

[27] A. Mastalir, Z. Kiraly, F. Berger, Appl. Catal. A 269 (2004) 161.

[28] A. J. Bird, D. T. Thompson, in: W. H. Jones (Ed.), Catalysis and Organic Synthesis, Academic Press, London, 1980.

Impact of the Silica Support Structure on Liquid-Phase Hydrogenation on Pd Catalysts

Joongjai Panpranot,*,† Kanda Pattamakomsan,† Piyasan Praserthdam,† and James G. Goodwin, Jr.‡

Center of Excellence on Catalysis and Catalytic Reaction Engineering, Department of Chemical Engineering, Chulalongkorn University, Bangkok 10330, Thailand, and Department of Chemical Engineering, Clemson University, Clemson, South Carolina 29634

The effect of the silica support structure on the characteristics and catalytic properties in liquid-phase hydrogenation of 1-hexene over two types of silica (amorphous SiO_2 and MCM-41) supported Pd catalysts was studied under mild conditions. The catalysts were characterized by atomic adsorption (AA), N_2 physisorption, X-ray diffraction (XRD), transmission electron microscopy (TEM), CO pulse chemisorption, and temperature-programmed reduction (TPR). The highest hydrogenation activity was found for the larger pore MCM-41 (d_{pore} = 9 nm) supported Pd catalysts. Use as a catalyst support of a smaller pore size MCM-41, a small-pore amorphous SiO_2, and a commercial large-pore SiO_2 led to lower Pd dispersions. The results suggest that Pd was inside the pores of the large-pore MCM-41 and SiO_2, and to a lesser extent for the small-pore MCM-41. However, almost no Pd appears to have been inside the pores of the small-pore SiO_2, the support with the greatest percent of pores <3 nm. There was no evidence of any pore diffusion limitations on reaction on any of the catalysts. TPR results showed that the PdO on smaller pore MCM-41 was not totally reduced at ambient temperature, resulting in a lower amount of active Pd^0 being available for catalyzing the reaction. Leaching of palladium into the reaction media occurred in all cases, and to a significant degree for several of the catalysts. However, the leaching of the Pd seemed to be primarily a function of Pd particle size, with larger particles being more susceptible, and probably particle location. This loss of Pd from the catalyst during reaction was most likely due to formation of palladium hydride, which is known to form more easily on larger Pd particles. Although activity decreased with every reaction cycle, the concentration of surface Pd metal atoms able to chemisorb CO reached a limiting value.

1. Introduction

In many organic syntheses, catalytic hydrogenation is carried out in a liquid phase using batch-type slurry processes and a supported noble metal (Pd, Pt, or Rh) catalyst.[1] Typical catalyst supports used in liquid-phase hydrogenation include silica[2−6] and alumina[7,8] and to a lesser extent carbon,[9] polymer,[10] and zeolite.[11,12] Hydrogenation is such a fast and highly exothermic reaction, severe diffusion limitations may be induced due to small pore diameters of the catalyst support. To overcome diffusion resistance, large-pore supports are usually preferred. Recently much attention has focused on the use of ordered mesoporous materials such as MCM-41,[13] SBA-x,[14] and HMS.[15] These materials have been shown to be suitable catalyst supports because they possess high BET surface areas, large pore volumes, and highly ordered pore structures with narrow pore size distributions in the range of 2−50 nm, depending on the synthesis chemicals and conditions. Shimazu et al. recently reported that MCM-41-supported Pd catalysts prepared by grafting of a palladium complex on MCM-41 exhibited high activity and high regioselectivity in the liquid-phase hydrogenation of dienes with −OH groups.[16]

Many publications have shown that a support can affect catalyst activity, selectivity, recycling, refining, materials handling, and reproducibility. For example, Shen et al.[17] reported that the nature of the supports (Al_2O_3, SiO_2, TiO_2, and ZrO_2) affects both the activity and selectivity of supported Pd catalysts in catalytic hydrogenation of carbon monoxide. Pinna et al.[18] compared Pd on activated carbon, silica, and alumina in the selective hydrogenation of benzaldehyde to benzyl alcohol. Pd/Al_2O_3 was found to exhibit a strong metal−support interaction, while Pd/C showed the highest activity for benzaldehyde hydrogenation. Choudary et al.[12] reported that Pd/MCM-41 is more active in partial hydrogenation of acetylenic compounds than Pd/Y-zeolite or Pd/K-10 clay.

Thus, in previous studies, the effects of different kinds of support materials on hydrogenation have been studied and compared. However, the effect of catalyst structure for similar support compositions has not been studied to much of a degree. For example, the effects of the pore size and pore structure of the same material in liquid-phase hydrogenation on activity and catalyst deactivation due to metal leaching remain unclear. In this study, the effects of the pore size and pore structure of the support silica were investigated in more detail in terms of metal dispersion and location on the support, catalyst reducibility, catalytic behavior, and catalyst durability in liquid-phase hydrogenation of 1-hexene under mild conditions at 1 atm of pressure, where the rate of reaction can be studied more easily.

* To whom correspondence should be addressed. Tel.: +66 (02)-218-6859. Fax: +66 (02)-218-6877. E-mail: joongjai.p@eng.chula.ac.th.

† Chulalongkorn University.

‡ Clemson University.

10.1021/ie0497947 CCC: $27.50
Published on Web 08/10/2004

2. Experimental Section

2.1. Preparation of Catalyst Supports. Pure silica MCM-41 with 3 nm pore diameters was prepared in the same manner as that of Cho et al.[19] using the gel composition of CTAB:0.3NH_3:4SiO_2:Na_2O:200H_2O, where CTAB denotes cetyltrimethylammonium bromide. Briefly, 20.03 g of colloidal silica Ludox AS 40% (Aldrich) was mixed with 22.67 g of 11.78% sodium hydroxide solution. Another mixture was prepared from 12.15 g of CTAB (Aldrich) in 36.45 g of deionized water and 0.4 g of an aqueous solution of 25% NH_3. Both of these mixtures were transferred into a Teflon-lined autoclave, stirred for 30 min, and then heated statically at 100 °C for 5 days. The pH of the gel was adjusted to 10.2 using 30% acetic acid every 24 h. The obtained solid material was filtered, washed with water until no base was detected, and then dried at 100 °C. The sample was then calcined in flowing nitrogen up to 550 °C (1−2 °C/min) and then in air at the same temperature for 5 h and is referred to in this paper as M-3nm. The larger pore MCM-41 (M-9 nm) was prepared by treating the M-3nm (before calcination) in an emulsion containing *N*,*N*-dimethyldecylamine (0.625 g in 37.5 g of water for each gram of MCM-41) for 3 days at 120 °C. This was washed thoroughly, dried, and calcined in flowing nitrogen up to 550 °C (1−2 °C/min) and then in air at the same temperature for 5 h to yield complete template removal.[20] The siliceous MCM-41 possesses an extremely low concentration of acid sites, which could be due to aluminum impurities in this material.[21] There would appear to be no effect of residual Br on surface acidity. Small-pore amorphous SiO_2 (chromatographic grade) with an average pore diameter of 3 nm and large-pore SiO_2 were obtained from Grace Davison and Strem Chemicals, respectively. The small- and large-pore silica are referred to in this paper as S-3nm and S-large, respectively.

2.2. Preparation of Supported Pd Catalysts. Supported Pd catalysts were prepared by the incipient wetness impregnation of the supports with an aqueous solution containing the desired amount of $Pd(NO_3)\cdot 2H_2O$ to yield a final loading of approximately 0.5 wt % Pd. The catalysts were dried overnight at 110 °C and then calcined in air at 500 °C for 2 h.

2.3. Catalyst Characterization. The bulk composition of palladium was determined using a Varian Spectra A800 atomic absorption spectrometer. The BET surface areas, pore volumes, average pore diameters, and pore size distributions of the catalysts were determined by N_2 physisorption using a Micromeritics ASAP 2000 automated system. Each sample was degassed under vacuum at <10 μmHg in the Micromeritics ASAP 2000 at 150 °C for 4 h prior to N_2 physisorption. The X-ray diffraction (XRD) spectra of the catalysts were measured from $2\theta = 20°$ to $2\theta = 80°$ using a Siemens D5000 X-ray diffractometer and Cu Kα radiation with a Ni filter. The palladium oxide particle size and distribution of palladium were observed using a JEOL-TEM 200CX transmission electron microscope operated at 100 kv. The catalyst sample was first suspended in ethanol using ultrasonic agitation for 10 min. The suspension was dropped onto a thin Formvar film supported on a copper grid and dried at room temperature before observation.

Relative percentages of palladium dispersion were determined by pulsing carbon monoxide over the reduced catalyst. Approximately 0.2 g of catalyst was placed in a quartz tube in a temperature-controlled oven. CO adsorption was determined by a thermal conductivity detector (TCD) at the exit. Prior to chemisorption, the catalyst was reduced in a flow of hydrogen (50 cm^3/min) at room temperature for 2 h. Then the sample was purged at this temperature with helium for 1 h. Carbon monoxide was pulsed at room temperature over the reduced catalyst until the TCD signal from a pulse was constant.

Table 1. N_2 Physisorption Results[a] for the Supports and Supported Pd Catalysts

	BET SA (m^2/g)	pore vol (cm^3/g)	avg pore diam (nm)
S-3nm	716	0.39	2.2
S-large	277	1.14	16.4
M-3nm	921	0.87	3.8
M-9nm	901	1.59	7.0
Pd/S-3nm	675	0.36	2.1
Pd/S-large	201	0.92	18.2
Pd/M-3nm	670	0.71	4.2
Pd/M-9nm	726	0.62	3.4

[a] The error of measurement was ±5%.

The temperature-programmed reduction (TPR) profiles of supported palladium catalysts were obtained using an in-house TPR system and a temperature ramp of 5 °C/min from 30 to 300 °C in a flow of 5% H_2 in argon. Approximately 0.20 g of a calcined catalyst was placed in a quartz tube in a temperature-controlled oven and connected to a TCD. The H_2 consumption was measured by analyzing the effluent gas with a thermal conductivity detector.

2.4. Liquid-Phase Hydrogenation. Liquid-phase hydrogenation of 1-hexene was carried out as a model reaction to compare the hydrogenation activity of the catalysts. The reaction was carried out at 25 °C and 1 atm in a stainless steel Parr autoclave. Approximately 1 g of supported Pd catalyst was placed into the autoclave. The system was purged with nitrogen to remove remaining air. The supported Pd catalyst was reduced with hydrogen at room temperature for 2 h. The reaction mixture composed of 15 mL of 1-hexene and 400 mL of ethanol was first placed in a 600 mL feed column. The reaction mixture was introduced into the reactor with nitrogen to start the reaction. The amount of hydrogen consumption was monitored every 5 min by noting the change in the pressure of hydrogen. The stirring rate used in this study was 1400 rpm. It was ensured that the reaction rate does not depend on the stirring rate. As also reported by others,[22−23] the activity of the stainless steel autoclave was observed and was found to be less than 10% of the catalyst activity. The activity of the autoclave was subtracted from the overall rate of reaction prior to reporting rate data. The liquid reactants, products, and headspace gases were analyzed by a gas chromatograph using a Shimazu GC-9A equipped with an FID detector. No reduction or decomposition of ethanol during the reaction was observed.

3. Results and Discussion

3.1. Catalyst BET Surface Area and Porosity. The BET surface areas, pore volumes, and average pore diameters of the original supports and the catalysts are given in Table 1. All silica supports except the commercial large-pore silica (S-large) possessed high BET surface areas of 716−921 m^2/g. Impregnation of silica with palladium followed by calcination resulted in

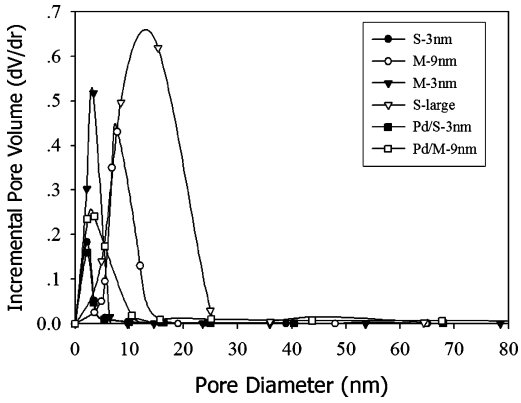

Figure 1. Pore size distribution of the original supports and several supported Pd catalysts.

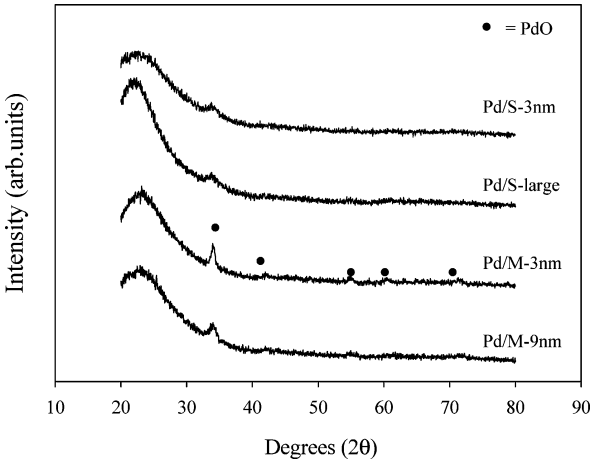

Figure 2. XRD patterns of the supported Pd catalysts.

significant decreases in the BET surface area and pore volume for all but one of the supports, suggesting that palladium was deposited in some of the pores. Only the small-pore amorphous SiO_2 (S-3nm) showed little loss of BET surface area after Pd loading. Figure 1 shows the pore size distribution of the four different silica supports and of the Pd/M-9nm and Pd/S-3nm catalysts in this study. A narrow pore size distribution was observed for all the catalyst supports except the commercial large-pore silica. Palladium loading did not appreciably change the average pore diameters of the SiO_2-supported and the small-pore-MCM-41-supported Pd catalysts. It did, however, significantly decrease that of the large-pore MCM-41 (Pd/M-9nm) catalyst.

3.2. Palladium Particle Size and Dispersion. The XRD patterns of the calcined supported Pd catalysts are presented in Figure 2. Diffraction peaks for palladium oxide (PdO) were detectable at $2\theta = 33.8°$ and less so at $2\theta = 42.0°$, 54.8°, 60.7°, and 71.4° in all the catalyst samples. The PdO crystallite sizes were calculated from the width of the XRD peak at $2\theta = 33.8°$ using the Scherrer equation[24] and are reported in Table 2. The PdO crystallite sizes were determined to be ca. 8−14 nm in the order Pd/M-3nm > Pd/S-large > Pd/S-3nm ≈ Pd/M-9nm.

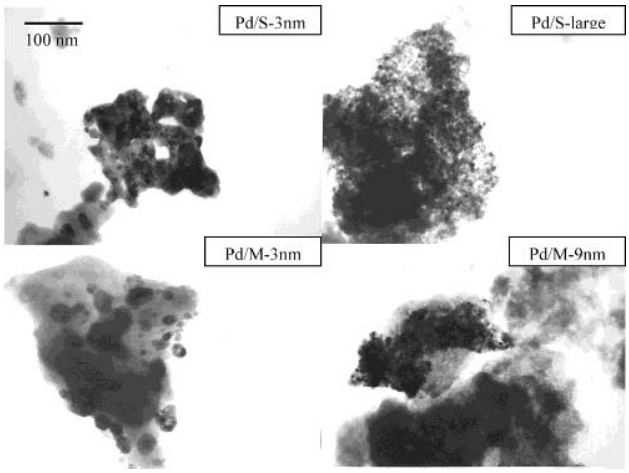

Figure 3. TEM micrographs of the supported Pd catalysts.

Transmission electron microscopy (TEM) micrographs were also taken to physically measure the size of the palladium oxide particles and/or palladium clusters. The average particle sizes of PdO were measured from TEM micrographs by averaging the diameters of 30−50 primary particles. The results were found to be in accordance with the XRD results. TEM micrographs of the calcined Pd supported catalysts are shown in Figure 3, and average PdO particle sizes determined are given in Table 2. Although TEM measurements were only done for a small portion of each catalyst, the results provide further evidence about the dispersion of the palladium. The differences in PdO particle sizes on different supports can be ascribed to differences induced by the support on the sintering of Pd during preparation and reaction.[12]

The amounts of CO chemisorption on the catalysts, the Pd dispersions, and the average Pd metal particle sizes determined from CO chemisorption are given in Table 2. The pulse CO chemisorption technique was based on the assumption that one carbon monoxide molecule adsorbs on one palladium site.[25−29] It was found that Pd/M-9nm catalyst exhibited the highest amount of CO chemisorption, whereas the other catalysts showed similar amounts of CO chemisorption. This was probably due to the dispersion of palladium being better on the larger pore MCM-41, as also shown above. The Pd dispersions were determined to be in the range of 4.4−12.0% in the descending order Pd/M-9nm > Pd/S-large > Pd/S-3nm > Pd/M-3nm. The average particle size for reduced Pd^0 was calculated to be in the range of 9.4−24.9 nm. These average Pd metal particle sizes

Table 2. CO Chemisorption Results and Sizes of PdO and Pd^0 Metal Particles

catalyst	PdO particle size (nm) XRD	PdO particle size (nm) TEM	CO chemisorption[a] (10^{18} molecules of CO/g of catalyst)	Pd dispersion[b] (%)	Pd^0 particle size[c] (nm)
Pd/S-3nm	7.8	8.0	1.29	6.5	17.2
Pd/S-large	10.8	10.0	1.22	7.3	15.3
Pd/M-3nm	14.2	12.8	1.20	4.4	24.9
Pd/M-9nm	9.1	6.7	2.10	12.0	9.4

[a] The error of measurement was ±5%. [b] Based on the total palladium loaded. An assumption of $CO/Pd_s^0 = 1$ was used, where Pd_s^0 is a reduced surface atom of Pd. [c] Based on $d = 1.12/D$ (nm),[25] where D = fractional metal dispersion.

calculated on the basis of CO chemisorption are not identical of course to the PdO particle sizes determined by XRD and TEM. The average Pd metal particle sizes on the reduced catalysts determined from CO chemisorption for Pd/S-3nm and Pd/M-3nm were found to be somewhat larger than the PdO particle sizes on the calcined catalysts determined from XRD and TEM. However, for Pd/S-large and Pd/M-9nm, the average metal and metal oxide particle sizes calculated from CO chemisorption, XRD, and TEM were found to be more consistent. Overestimation of Pd metal particle sizes by CO chemisorption for the catalysts with small pores (Pd/S-3nm and Pd/M-3nm) could have possibly been due to (a) partial blockage of CO adsorption as a result of pore blockage by agglomeration of metal particles[30] and (b) localized destruction of the well-defined pore structure, forming cracks and holes where larger metal particles could form and chemisorption would also be restricted,[31] or (c) chemisorption suppression due to strong support−metal interactions.[32] Chemisorption suppression may relate to a decrease in the kinetics of chemisorption (resulting in poor uptake at a given temperature) as a result of it becoming more highly activated.

3.3. Pd Location. For Pd/S-large, the XRD and TEM results for PdO and CO chemisorption for the reduced Pd^0 gave particle sizes small enough to exist within the large pores of that support. The pores were large enough that the metal particles did not block the pore structure much, resulting in little decrease in BET surface area and pore volume. This large-pore-SiO_2-supported catalyst apparently had little trouble in adsorbing the Pd precursor solution in its large pores during the incipient wetness impregnation and in accommodating the Pd particles formed, with a resulting loss of BET surface area and pore volume. For Pd/M-9nm, the decrease in BET pore diameter upon loading with Pd suggests that the pores were significantly blocked up. This is also very evident in the pore diameter distribution change seen in Figure 1. On the basis of XRD and TEM of PdO and CO chemisorption on the reduced Pd^0 metal, the metal particles were small enough such that they could be significantly deposited in the mesopores of this material.

In the case of Pd/S-3nm and Pd/M-3nm, PdO particles were found by XRD and TEM to be much larger than the average pore diameters. CO chemisorption results confirm the large metal particles existing on the reduced catalysts. For S-3nm, addition of Pd did not significantly affect the average pore diameter, and the pore diameter distribution (Figure 1) remained identical. Therefore, evidence suggests that most of the Pd particles were on the outside support surfaces of Pd/S-3nm and not in the micropores, perhaps due to a difficulty for the preparation solution to penetrate these small pores. For Pd/M-3nm, CO chemisorption determined larger average particle sizes than XRD and TEM partly because of the less than 100% reduction for Pd on this catalyst as determined by TPR and possibly because of some blockage of the metal surfaces of metal particles located inside the micropores. As can be seen in Figure 1, M-3nm had many pores with much larger diameters than those of S-3nm. This must have made it possible for Pd particles to be deposited in part inside the larger of these pores.

3.4. Catalyst Reducibility. The reducibility of the catalysts is important since the active phase for hydrogenation is the metallic Pd^0 phase. Figure 4 shows the TPR profiles of different supported Pd catalysts. It was found that, in most cases, PdO particles were reduced readily to PdH_2 at ambient temperature once hydrogen was introduced into the system, typical for supported Pd catalysts prepared from palladium nitrate.[33] A significant negative peak at ca. 75−80 °C was observed for all the catalysts; this peak can be attributed to the decomposition of PdH_2.[34] Koh et al.[35] has referred to a private communication with G. C. Bond that about 70% of the PdO contained in MCM-41-supported catalysts can be reduced at subambient temperature and the other 30% is reducible by 50 °C. However, no TPR profile of Pd/MCM-41 was shown. From our results, a small reduction peak at ca. 48 °C was observed for Pd/M-3nm and is attributed to a portion of the PdO that could not be reduced at ambient temperature. It has previously been reported that there is a stronger metal−support interaction between metal and an MCM-41 support when the pore size of that support is very small (i.e., 3 nm).[36] In the case of amorphous silica (SiO_2), there would appear to be no difference in the metal−support interaction (Pd−SiO_2) between the small- and large-pore supports. It should also be noted that large-pore-MCM-41-supported Pd catalysts exhibited TPR profiles similar to those of SiO_2-supported Pd catalysts.

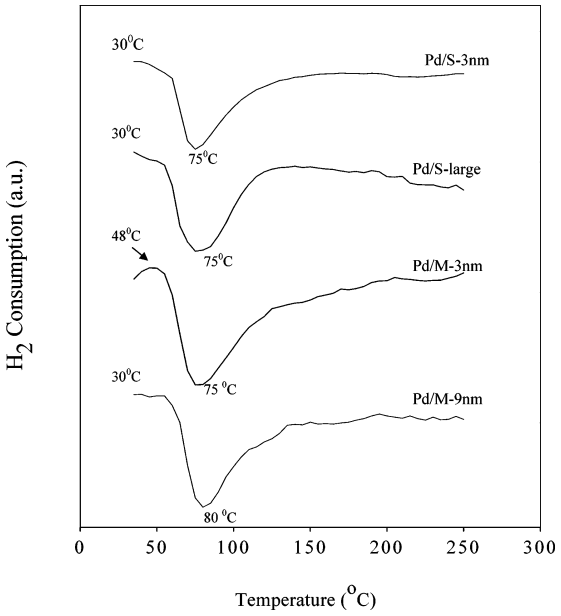

Figure 4. TPR profiles of the supported Pd catalysts.

3.5. Catalytic Behavior. The kinetics of liquid-phase hydrogenation of 1-hexene was studied using the rate of hydrogen consumption.[3−5,12,37,38] The rates of H_2 consumption versus time-on-stream for the supported Pd catalysts are shown in Figure 5. The slope of the line at the origin represents the initial rate of reaction and the rate constant assuming zero-order dependence of the reaction on hydrogen.[12,39] The rate constants for liquid-phase hydrogenation of 1-hexene at 25 °C of the supported Pd catalysts and the turnover frequencies are reported in Table 3. The activities of the catalysts were found to be in the order Pd/M-9nm > Pd/M-3nm ≈ Pd/S-large > Pd/S-3nm. The turnover frequencies (TOFs) were calculated using the number of surface metal atoms measured by pulse CO chemisorption. For a given silica type, larger pore supported Pd catalysts were more active than smaller pore supported ones. However, on the basis of TOF, there was little difference in the rate of reaction on the different catalysts. Given the wide

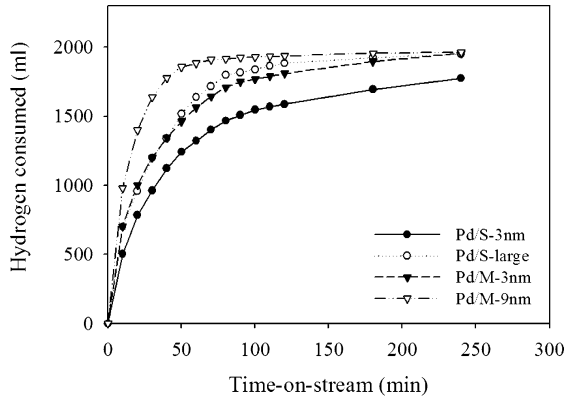

Figure 5. Liquid-phase hydrogenation activity of the supported Pd catalysts (reaction conditions: 25 °C, 1 atm, and 1-hexene/ethanol = 15/400 mL).

Table 3. Catalytic Activity of Different Supported Pd Catalysts in Liquid-Phase Hydrogenation of 1-Hexene at 25 °C and 1 atm

catalyst	rate constant[a] (10^3 (mol/min)/g of catalyst)	TOF[b] (s^{-1})
Pd/S-3nm	2.45	19
Pd/S-large	3.40	29
Pd/M-3nm	3.41	28
Pd/M-9nm	4.75	23

[a] Based on the initial rate. [b] Based on the initial rate of reaction and number of active sites measured by CO chemisorption.

Table 4. Metal Leaching during Reaction[b]

catalyst	Pd loading[a] (wt %) before	Pd loading[a] (wt %) after	% metal loss
Pd/S-3nm	0.35	0.15	57
Pd/S-large	0.29	0.18	38
Pd/M-3nm	0.48	0.32	33
Pd/M-9nm	0.33	0.31	6

[a] Determined by atomic adsorption. The error of measurement was ±5%. [b] After 5 h batch hydrogenation of 1-hexene at 25 °C and 1 atm.

range of pore diameters and the fact that, for S-large and M-9 nm, the majority of Pd particles were inside the support pores, it can be concluded that the internal resistance due to diffusion within the pores of the reactant species did not have any influence on the catalytic activity of the catalysts. However, the rate may have been limited by the rate of dissolution and the solubility of hydrogen in the liquid phase where the catalyst was located.

3.6. Catalyst Durability. The actual amounts of palladium loading before and after reaction were determined by atomic absorption spectroscopy and are given in Table 4. Before reaction, palladium loading on the catalyst samples was 0.29−0.48 wt %. After 5 h batch hydrogenation reactions of 1-hexene, palladium loading on the catalysts had decreased to 0.15−0.32 wt %. This indicates that leaching of palladium occurred during reaction. Leaching of active metal is one of the main causes of catalyst deactivation in liquid-phase reaction. It depends on the reaction medium (pH, oxidation potential, chelating properties of the molecules) and the bulk and surface properties of the metal.[40] In this study, the order of the percentage of palladium leached was Pd/S-3nm > Pd/S-large > Pd/M-3nm > Pd/M-9nm, where Pd/M-9nm showed almost no leaching of palladium into the reaction media within experimental error. It would appear that Pd/M-9nm is the only catalyst with Pd supported in relatively small pores and is also the catalyst with the smallest Pd particles. Thus, it can be suggested that metal loss is affected by metal particle size and whether the Pd particles are located on the external surface or in large pores (greater loss) or in mesopores (less loss).

The mechanism of metal leaching involves usually metal compounds that are formed and are soluble in the reaction mixture. Since it is unlikely that 1-hexene forms a compound with Pd at room temperature, unless it is some hydridoorganic complex, it is likely that palladium hydride formation is the cause of metal loss. It is well-known that Pd particles are able to absorb H_2 within their structure to form a palladium β-hydride phase. A number of publications[17,41] have reported that formation of palladium hydride depends on the particle size of palladium; larger Pd particles more easily form palladium hydride, whereas smaller Pd particles may be unable to form the palladium β-hydride phase. Under certain conditions, the palladium β-hydride phase can appear as a soft material with higher mechanical abrasion.[42] This may also be a reason that larger Pd particles on the external surfaces of the catalyst granules form the palladium β-hydride phase that is lost (leached) from the catalysts. However, it should be noted that Pd/S-large also lost a significant amount of Pd during reaction, even though most of its Pd particles can be assumed to have been inside its large pores and, therefore, not susceptible to physical abrasion. Thus, it is more likely that a soluble Pd compound was formed on the larger Pd particles. It should be noted that the leached Pd was not taken into account in the analysis of catalyst activity since palladium β-hydride is expected to have a catalytic activity different from that of metallic palladium.[43] In addition, the initial rate and TOF were determined early in the reaction when the amount of metal lost would have been minimal.

The durabilities of the catalysts under repeated catalytic cycles were tested on Pd/M-3nm catalyst since it exhibited a significant amount of metal loss during reaction. The experiment was carried out at 25 °C and atmospheric pressure by injecting 7.5 mL of 1-hexene at 2 h intervals. After different numbers of reaction cycles (0, 1, 2, or 3), the used catalyst was filtered out, dried at room temperature, and calcined in air at 500 °C for 2 h to remove any carbon deposited. Then CO chemisorption was performed on the used catalysts following the same procedure as for the fresh catalysts. Figure 6 shows the initial reaction rates and the number of palladium active sites as measured by CO chemisorption versus the number of reaction cycles undergone. It was found that the reaction rate decreased with each cycle. This might be due to leaching of palladium from the supports and/or a decrease in the amounts of palladium active sites due to sintering of the palladium.[3,41] However, CO chemisorption after recalcination at 500 °C in a flow of air followed by rereduction showed complete retention of palladium CO chemisorption sites after one cycle of reaction.

Finally, as mentioned above, it is likely that both the Pd particle size and location have effects on Pd leaching during this reaction. Thus, although Pd/M-3 nm had many large particles, there must have been many smaller ones located within the mesopores >3 nm in diameter, and this resulted in lower amounts of Pd being leached out. The leaching for Pd/S-3nm was the

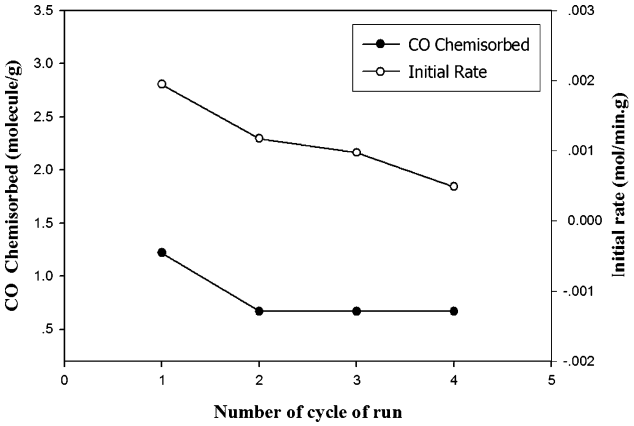

Figure 6. Stability of Pd/M-3nm catalyst as a function of the number of reaction cycles (reaction conditions: 25 °C, 1 atm, and 1-hexene/ethanol = 15/400 mL).

highest because all the Pd particles were large and existed on the outer surfaces of the silica granules. Pd/S-large probably had a relatively large Pd loss because it had large Pd particles in very large pores. The best catalyst in retaining Pd during reaction was Pd/M-9nm, which had most of the Pd in the moderately sized mesopores. It can be speculated that pore size may affect particle geometry and, hence, palladium hydride formation.

4. Conclusions

In this paper we have reported on the effect of the silica support structure (MCM-41 and amorphous SiO_2) on the catalyst and reaction properties of supported Pd. For the larger pore supports (S-large and M-9nm), Pd particles likely formed primarily in the pores, whereas use of smaller pore supports resulted in Pd particles primarily on the outside surface of the catalyst granules (S-3nm) or both inside and outside the support pores (M-3nm). All the catalysts exhibited similar TOFs for the liquid-phase hydrogenation of 1-hexene. Under the conditions used, there was no evidence for mass-transfer limitations in the liquid phase. All but one catalyst (Pd/M-9nm) showed significant loss of Pd during reaction, probably as a result of palladium hydride formation. The Pd particle size appeared to strongly determine this metal loss during reaction. However, it is also likely that the location on the silica support also played an important role. The results provide a cautionary note to the use of SiO_2-supported Pd for liquid-phase organic hydrogenation since there can be so much metal loss during reaction. The results for Pd/M-9nm suggest a means to minimize such loss.

Acknowledgment

The financial support of the Thailand Research Fund (TRF) and TJTTP-JBIC are gratefully acknowledged. We also thank Professor Abdelhamid Sayari, University of Ottawa, Canada, and Dr. Aticha Chaisuwan, Chulalongkorn University, Thailand, for assistance with the MCM-41 preparation.

Literature Cited

(1) Rylander, P. N. *Hydrogenation Methods*; Academic Press: New York, 1985.

(2) Guczi, L.; Horvath, A.; Beck, A.; Sarkany, A. Controlling Metal Particle Size in Preparation of Pd/SiO_2 Catalysts. *Stud. Surf. Sci. Catal.* **2003**, *145*, 351.

(3) Dominguez-Quintero, O.; Martinez, S.; Henriquez, Y.; D'Ornelas, L.; Krentzien, H.; Osuna, J. Silica-Supported Palladium Nanoparticles Show Remarkable Hydrogenation Catalytic Activity. *J. Mol. Catal. A* **2003**, *197*, 185.

(4) Stanger, K. J.; Tang, Y.; Anderegg, J.; Angelici, R. J. Arene Hydrogenation using Supported Rhodium Metal Catalysts Prepared from $[Rh(COD)H]_4$, $[Rh(COD)_2+BF_4$, and $[Rh(COD)Cl]_2$ Adsorbed on SiO_2 and Pd-SiO_2. *J. Mol. Catal. A.* **2003**, *202*, 147.

(5) Palinko, I. Effects of Surface Modifiers on the Liquid-Phase Hydrogenation of Alkenes over Silica-Supported Platinum, Palladium, and Rhodium Catalysts I. Quinoline and Carbon Tetrachloride. *Appl. Catal., A* **1995**, *126*, 39.

(6) Lopez, T.; Asomoza, M.; Bosch, P.; Garcia-Figueroa, E.; Gomez, R. Spectroscopic Characterization and Catalytic Properties of Sol-Gel Palladium/Silica Catalysts. *J. Catal.* **1992**, *138*, 463.

(7) Borszeky, K.; Mallet, T.; Eschiman, R.; Schweizer, W. B.; Baiker, A. Enantioselective Hydrogenation of Pyruvic Acid to Alanine on Pd/Alumina. *J. Catal.* **1996**, *161*, 451.

(8) L'Argentiere, P. L.; Liprandi, D. A.; Cagnola, E. A.; Figoli, N. S. $[PdCl_2(NH_2)(CH_2)_{12}(CH_3)_2]$ Supported on γ-Al_2O_3 as Catalyst for Selective Hydrogenation. *Catal. Lett.* **1997**, *44*, 101.

(9) Jackson, S. D.; Shaw, L. A. The Liquid Phase Hydrogenation of Phenyl Acetylene and Styrene on a Palladium/Carbon Catalyst. *Appl. Catal., A* **1996**, *134*, 91.

(10) Mathew, J. P.; Srinivasan, M. Photoelectron-Spectroscopy (XPS) Studies on Some Palladium Catalysts. *Eur. Polym. J.* **1995**, *31*, 835.

(11) Creyghton, E. J.; Downing, R. S. Shape-Selective Hydrogenation and Hydrogen Transfer Reactions over Zeolite Catalysts. *J. Mol. Catal. A* **1998**, *134*, 47.

(12) Choudary, B. M.; Kantam, M. L.; Reddy, N. M.; Rao, K. K.; Haritha, Y.; Bhaskar, V.; Figueras, F.; Tuel, A. Hydrogenation of Acetylenics by Pd-Exchange Mesoporous Materials. *Appl. Catal., A* **1999**, *181*, 139.

(13) Beck, J. S.; Vartuli, J. C.; Roth, W. J.; Leonowicz, M. E.; Kresge, C. T.; Schmitt, K. D.; Chu, C. T.-W.; Olson, D. H.; Sheppard, E. W.; McCullen, S. B.; Higgins, J. B.; Schlenker, J. L. A New Family of Mesoporous Molecular Sieves Prepared with Liquid Crystal Templates. *J. Am. Chem. Soc.* **1992**, *114*, 10834.

(14) Zhao, D.; Feng, J.; Huo, Q.; Melosh, N.; Frederickson, G. H.; Chmelka, B. F.; Stucky, G. C. Triblock Copolymer Syntheses of Mesoporous Silica with Periodic 50 to 300 Angstrom Pores. *Science* **1998**, *279*, 548.

(15) Tanev, P. T.; Pinnavaia, T. J. Biomimetic Templating of Porous Lamellar Silicas by Vesicular Surfactant Assemblies. *Science* **1996**, *271*, 1267.

(16) Shimazu, S. B.; Ichiku, N.; Uematsu, T. Regioselective Hydrogenation of Dienes Catalyzed by Palladium-Aminosilane Complexes Grafted on MCM-41. *J. Mol. Catal.* **2002**, *182*, 343.

(17) Shen, W. J.; Okumura, M.; Matsumura, Y.; Haruta, M. The Influence of the Support on the Activity and Selectivity of Pd in CO Hydrogenation. *Appl. Catal., A* **2001**, *213*, 225.

(18) Pinna, F.; Menegazzo, F.; Signoretto, M.; Canton, P.; Fagherazzi, G.; Pernicone, N. Consecutive Hydrogenation of Benzaldehyde over Pd Catalysts-Influence of Supports and Sulfur Poisoning. *Appl. Catal., A* **2001**, *219*, 195.

(19) Cho, D. H.; Chang, T. S.; Ryu, S. K.; Lee, Y. K. Characterization and Catalytic Activities of Mo/MCM-41. *Catal. Lett.* **2000**, *64*, 227.

(20) Kleitz, F.; Schmidt, W.; Schuth, F. Calcination Behavior of Different Surfactant Templated Mesostructured Silica Materials. *Microporous Mesoporous Mater.* **2003**, *65*, 1.

(21) Zholobenko, V. L.; Plant, D.; Evans, A. J.; Holmes, S. M. Acid Sites in Mesoporous Materials: a DRIFTS Study. *Microporous Mesoporous Mater.* **2001**, *44*−*45*, 793.

(22) Englisch, M.; Ranade, V. S.; Lercher, J. A. Liquid-Phase Hydrogenation of Crotonaldehyde over Pt/SiO_2 Catalysts. *Appl. Catal., A* **1997**, *163*, 111.

(23) Tahara, K.; Tsuji, H.; Kimura, H.; Okazaki, T.; Itoi, Y.; Nishiyama, S.; Tsuruya, S.; Masai, M. Liquid-Phase Hydrogenation of Dicarboxylates Catalyzed by Supported Ru-Sn Catalysts. *Catal. Today* **1996**, *28*, 267.

(24) Klug, H. P.; Alexander, L. E. *X-Ray Diffraction Procedures For Polycrystalline Amorphous Materials*, 2nd ed.; Wiley: New York, 1974.

(25) Mahata, N.; Vishwanathan, V. Influence of Palladium Precursors on Structural Properties and Phenol Hydrogenation Characteristics of Supported Palladium Catalysts. *J. Catal.* **2000**, *196*, 262.

(26) Ali, S. H.; Goodwin, J. G., Jr. SSITKA Investigation of Palladium Precursor and Support Effects on CO Hydrogenation over Supported Pd Catalysts. *J. Catal.* **1998**, *176*, 3.

(27) Sales, E. A.; Bugli, G.; Ensuque, A.; Mendes, M. J.; Bozon-Verduraz, F. Palladium Catalysts in the Selective Hydrogenation of Hexa-1,5-diene and Hexa-1,3-diene in the Liquid Phase. Effect of Tin and Silver Addition-Part 1. Preparation and Characterization: From the Precursor Species to the Final Phases. *Phys. Chem. Chem. Phys.* **1999**, *1*, 491.

(28) Sarkany, A.; Zsoldos, Z.; Furlong, B.; Hightower, J. W.; Guczi, L. Hydrogenation of 1-Butene and 1,3 Butadiene Mixture over Pd/ZnO Catalysts. *J. Catal.* **1993**, *141*, 566.

(29) Nag, N. K. A Study on the Dispersion and Catalytic Activity of γ-Alumina Supported Palladium Catalysts. *Catal. Lett.* **1994**, *24*, 37.

(30) Verdonck, J. J.; Jacobs, P. A.; Genet, M.; Poncelet, G. Redox Behavior of Transition Metal Ions in Zeolites. Part 8. Characterization of a Ruthenium Metal Phase in NaY Zeolite. *J. Chem. Soc., Faraday Trans.* **1980**, *76*, 403.

(31) Gustafson, B. L.; Lunsford, J. H. The Catalytic Reactions of Carbon Monoxide and Water over Ruthenium in a Y-Type Zeolite. *J. Catal.* **1982**, *74*, 393.

(32) Tauster, S. J.; Fung, S. C.; Garten, R. L. Strong Metal-Support Interactions. Group 8 Noble Metals Supported on TiO_2. *J. Am. Chem. Soc.* **1978**, *100*, 170.

(33) Shen, W. J.; Ichihashi, Y.; Ando, H.; Okamura, M.; Haruta, M.; Matsumura, Y. Influence of Palladium Precursors on Methanol Synthesis from CO Hydrogenation over Pd/CeO_2 Catalysts Prepared by Deposition-Precipitation Method. *Appl. Catal., A* **2001**, *217*, 165.

(34) Cubeiro, M. L.; Fierro, J. L. G. Partial Oxidation of Methanol over Supported Palladium Catalysts. *Appl. Catal., A* **1998**, *168*, 307.

(35) Koh, C. A.; Nooney, R.; Tahir, S. Characterization and Catalytic Properties of MCM-41 and Pd/MCM-41 Materials. *Catal. Lett.* **1997**, *47*, 199.

(36) Panpranot, J.; Goodwin, J. G., Jr.; Sayari, A. Synthesis and Characteristics of MCM-41 Supported CoRu Catalysts. *Catal. Today* **2002**, *77*, 269.

(37) Dalal, M. K.; Ram, R. N. Hydrogenation of 1-Hexene using Polymer Supported Pd(II) Complex Catalyst. *Eur. Polym. J.* **1997**, *33*, 1495.

(38) Li, H.; Xu, Y. Liquid-Phase Benzene Hydrogenation to Cyclohexane over Modified Ni−P Amorphous Catalysts. *Mater. Lett.* **2001**, *51*, 101.

(39) Sales, E. A.; Mendes, M. D.; Bozon-Verduraz, F. Liquid Phase Selective Hydrogenation of Hexa-1,5-diene and Hexa-1,3-diene on Palladium Catalysts. Effect of Tin and Silver Addition. *J. Catal.* **2000**, *195*, 96.

(40) Besson, M.; Gallezot, P. Deactivation of Metal Catalysts in Liquid Phase Organic Reactions. *Catal. Today* **2003**, *81*, 547.

(41) Neri, G.; Musolino, M. G.; Milone, C.; Pietropaolo, D.; Glavagno, S. Particle Size Effect in the Catalytic Hydrogenation of 2,4-Dinitrotoluene over Pd/C Catalysts. *Appl. Catal., A* **2001**, *208*, 307.

(42) Albers, P.; Pietsch, J.; Parker, S. F. Poisoning and Deactivation of Palladium Catalyst. *J. Mol. Catal. A* **2001**, *173*, 275.

(43) Walter, J.; Heiermann, J.; Dyker, G.; Hara, S.; Shioyama, H. Hexagonal or Quasi Two-Dimensional Palladium Nanoparticles-Tested at the Heck Reaction. *J. Catal.* **2000**, *189*, 449.

Received for review March 16, 2004
Revised manuscript received May 25, 2004
Accepted July 1, 2004

IE0497947

Available online at www.sciencedirect.com
SCIENCE DIRECT®
Catalysis Communications 5 (2004) 583–590
CATALYSIS COMMUNICATIONS
www.elsevier.com/locate/catcom

A comparative study of Pd/SiO_2 and Pd/MCM-41 catalysts in liquid-phase hydrogenation

Joongjai Panpranot [a,*], Kanda Pattamakomsan [a], James G. Goodwin Jr. [b], Piyasan Praserthdam [a]

[a] *Center of Excellence on Catalysis and Catalytic Reaction Engineering, Department of Chemical Engineering, Chulalongkorn University, Bangkok 10330, Thailand*
[b] *Department of Chemical Engineering, Clemson University, Clemson, SC 29634, USA*

Received 1 March 2004; revised 30 June 2004; accepted 9 July 2004
Available online 23 August 2004

Abstract

The characteristics and catalytic properties of Pd/MCM-41 and Pd/SiO_2 were investigated and compared in terms of Pd dispersion, catalytic activities for liquid-phase hydrogenation of 1-hexene, and deactivation of the catalysts. High Pd dispersion was observed on Pd/MCM-41-large pore catalyst while the other catalysts showed relatively low Pd dispersion due to significant amount of Pd being located out of the pores of the supports. Based on CO chemisorption results, the catalyst activities seemed to be primarily related to the Pd dispersion and not to diffusion limitation since TOFs were nearly identical for all the catalysts used in this study. In all cases, leaching and sintering of Pd caused catalyst deactivation after 5-h batch reaction. However, compared to Pd/SiO_2 with a similar pore size, Pd/MCM-41 exhibited higher hydrogenation activity and lower amount of metal loss.

Keywords: Liquid phase hydrogenation; Pd/MCM-41; Pd/SiO_2; 1-Hexene hydrogenation

1. Introduction

Supported Pd catalysts are widely used in liquid-phase hydrogenation for many important organic transformations [1]. Common catalyst supports include activated carbons [2,3], silicas [4,5], aluminas [6,7], and to a lesser extent, polymers [8], and zeolites [9]. It is know that a support can affect catalyst activity, selectivity, recycling, refining, materials handling, and reproducibility. For examples, Shen et al. [10] reported the effect of the nature of the supports (Al_2O_3, SiO_2, TiO_2, and ZrO_2) on both activity and selectivity of supported Pd catalysts in catalytic hydrogenation of carbon monoxide. Pinna et al. [11] compared Pd on activated carbon, silica, and alumina in the selective hydrogenation of benzaldehyde to benzyl alcohol. Pd/Al_2O_3 was found to exhibit strong metal–support interaction while Pd/C showed the highest activity for benzaldehyde hydrogenation. Besides the nature of the support, support structure can also affect catalyst performance. Choudary et al. [9] reported that Pd/MCM-41 is more active in partial-hydrogenation of acetylenic compounds than Pd/Y-zeolite or Pd/K-10 clay.

Ordered mesoporous silicas such as MCM-41 [12,13], SBA-x [14], and HMS [15], have been shown to be suitable catalyst supports. These mesoporous materials possess high BET surface areas, large pore volumes, and highly ordered pore structures with narrow pore size distributions in the range of 2–50 nm, depending on synthesis chemicals and conditions. Pt/MCM-41 has been

* Corresponding author. Tel.: +66 02 218 6859; fax: +66 02 218 6877.
E-mail address: joongjai.p@eng.chula.ac.th (J. Panpranot).

1566-7367/$ - see front matter © 2004 Elsevier B.V. All rights reserved.
doi:10.1016/j.catcom.2004.07.008

reported to exhibit high activity for the hydrogenation of aromatics in diesel fuels [16]. Co–Mo/MCM-41 was found to be more active than the conventional Co–Mo/Al_2O_3 catalyst for hydrodesulfurization [17]. For liquid phase reaction, Shimazu et al. [18] recently reported that MCM-41-supported Pd catalysts prepared by grafting of a palladium complex on MCM-41 exhibited high activity and high regioselectivity in the hydrogenation of dienes with –OH groups.

In this study, we compare the characteristics and catalytic properties of Pd/SiO_2 and Pd/MCM-41 with 2 different pore sizes (small and large pore). The effects of silica-structure and pore size of the silica supports were investigated in terms of metal dispersion, catalytic activity in liquid-phase hydrogenation, and deactivation due to metal leaching. These results supply useful information on the role of support porosity and type of silica used in supported Pd catalysts for liquid phase hydrogenation reactions.

2. Experimental

2.1. Preparation of supported Pd catalysts

Pure silica MCM-41 with 3 nm pore diameters was prepared in the same manner as that of Cho et al. [19] using the gel composition of CTABr:0.3 NH_3:4 SiO_2:Na_2O:200 H_2O, where CTABr denotes cetyltrimethyl ammonium bromide. Briefly, 20.03 g of colloidal silica Ludox AS 40% (Aldrich) was mixed with 22.67 g of 11.78% sodium hydroxide solution. Another mixture comprised of 12.15 g of CTABr (Aldrich) in 36.45 g of deionized water, and 0.4 g of an aqueous solution of 25% NH_3. Both of these mixtures were transferred into a Teflon lined autoclave, stirred for 30 min, then heated statically at 100 °C for 5 days. The obtained solid material was filtered, washed with water until no base was detected and then dried at 100 °C. The sample was then calcined in flowing nitrogen up to 550 °C (1–2 °C/min), then in air at the same temperature for 5 h, and is referred to in this paper as small pore MCM-41. The larger pore MCM-41 was prepared by treating the MCM-41-small pore (before calcination) in an emulsion containing *N*,*N*-dimethyldecylamine (0.625 g in 37.5 g of water for each gram of MCM-41) for 3 days at 120 °C. This was washed thoroughly, dried, and calcined in flowing nitrogen up to 550 °C (1–2 °C/min), then in air at the same temperature for 5 h. This support is referred to in this paper as large pore MCM-41. The amorphous SiO_2-small pore (chromatographic grade) and SiO_2-large pore were obtained commercially from Grace Davison and Strem chemicals, respectively.

Supported Pd catalysts were prepared by the incipient wetness impregnation of the supports with an aqueous solution containing the desired amount of Pd nitrate dehydrate to yield a final loading of approximately 0.5 wt% Pd. The catalysts were dried overnight at 110 °C and then calcined in air at 500 °C for 2 h.

2.2. Catalyst characterization

The bulk composition of palladium was determined using a Varian Spectra A800 atomic adsorption spectrometer. The BET surface area of the catalysts were determined by N_2 physisorption using a Micromeritics ASAP 2000 automated system. Each sample was degassed in the Micromeritics ASAP 2000 at 150 °C for 4 h prior to N_2 physisorption. The XRD spectra of the catalysts were measured using a SIEMENS D5000 X-ray diffractometer and Cu Kα radiation with a Ni filter in the 2–10° or 20–80° 2θ angular regions.

Catalyst particle morphology was obtained using a JEOL JSM-35CF scanning electron microscope operated at 20 kV. The palladium oxide particle size and distribution of palladium was observed using a JEOL-TEM 200CX transmission electron microscope operated at 100 kV. The catalyst sample was first suspended in ethanol using ultrasonic agitation for 10 min. The suspension was dropped onto a thin Formvar film supported on a copper grid and dried at room temperature before TEM observation.

Relative percentages of palladium dispersion were determined by pulsing carbon monoxide over the reduced catalyst. Approximately 0.2 g of catalyst was placed in a quartz tube, incorporated in a temperature-controlled oven and connected to a thermal conductivity detector (TCD). Prior to chemisorption, the catalyst was reduced in a flow of hydrogen (50 cc/min) at room temperature for 2 h. Then the sample was purged with helium for 1 h. Carbon monoxide was pulsed at room temperature over the reduced catalyst until the TCD signal from the pulse was constant.

2.3. Liquid-phase hydrogenation

Liquid-phase hydrogenation reactions were carried out at 25 °C and 1 atm in a stainless steel Parr autoclave. Approximately 1 g of supported Pd catalyst was placed into the autoclave. The system was purged with nitrogen to remove remaining air. The supported Pd catalyst was reduced with hydrogen at room temperature for 2 h. The reaction mixture composed of 15 ml of 1-hexene and 400 ethanol was first kept in a 600 ml feed column. The reaction mixture was introduced into the reactor with nitrogen to start the reaction. The content of hydrogen consumption was monitored every 5 min by noting the change in pressure of hydrogen.

3. Results and discussion

3.1. Catalytic activities for liquid phase hydrogenation of 1-hexene

Liquid-phase hydrogenation of 1-hexene was carried out as a model reaction to compare the hydrogenation activity of the MCM-41- and SiO_2-supported Pd catalysts. Mild conditions were chosen because rate of reaction can be studied more easily. In terms of kinetics study, the effects of 1-hexene concentration (0.1–0.3), hydrogen pressure (1–2 bar), and temperature (25–40 °C) were investigated. The initial rate of hydrogenation of 1-hexene was found to be independent on both 1-hexene concentration and hydrogen pressure. The apparent activation energy calculated from the Arrhenius plot was found to be 41 kJ/mol. The kinetics study of liquid phase hydrogenation using rate of hydrogen consumption have also been reported in other research investigations [9,20]. The slope of the line at the origin represents the initial rate of the reactions and the rate constant assuming zero order dependence of reaction on hydrogen [9,20,21]. The rate constant of the different supported Pd catalysts in liquid phase hydrogenation of 1-hexene at 25 °C and the corresponding turnover frequencies (TOFs) are reported in Table 1. The activity of the catalysts were found to be in the order of Pd/MCM-41-large pore > Pd/MCM-41-small pore ≈ Pd/SiO_2-large pore > Pd/SiO_2-small pore. The TOFs were calculated based on the CO chemisorption data (Table 2). Given that in all cases the support was silica, albeit in slightly different forms, it is not surprising that specific activities in the form of TOFs were so similar. Since the TOFs were similar but Pd particle locations so disparate: on the outside of the silica granules for Pd/SiO_2-small pore vs. inside mesopores for Pd/MCM-41-large pore, etc. (based on the average particle sizes of PdO measured from XRD and TEM), it would appear that there were no pore diffusion effects on reaction rate. However, this does not mean that there might not have been some limitations in the mass transfer of hydrogen from the gas phase to the liquid phase, given that hydrogenation is such a fast reaction on noble metals. However, we did not detect any mass transfer limitations due to pore diffusion. This is contrary to the effect of pore size on the liquid-phase diffusion resistance reported in the literature for other catalyst systems [22,23] The structure of MCM-41, however, may promote the reaction by affecting the crystal structure of the supported Pd to form more active centers for Pd catalysts [24].

3.2. Catalyst characterization before and after reaction

The characteristics of the catalysts before and after reaction were obtained using various analysis tools such

Table 1
Catalyst characteristics and liquid phase hydrogenation activity

Catalyst	BET surface area[a] (cm^3/g)			PdO particle size[c] (nm)		Rate constant $\times 10^3$ (mol/min g cat.)	TOFs[d] (s^{-1})
	Support	Fresh	Spent[b]	Fresh	Spent		
Pd/SiO_2-small pore	716	675	343	7.8	13.8	2.45	19
Pd/SiO_2-large pore	277	201	191	10.8	21.9	3.40	29
Pd/MCM-41-small pore	921	670	377	14.2	16.1	3.41	28
Pd/MCM-41-large pore	901	726	546	9.1	18.0	4.75	23

[a] Error of measurement was ±5%.
[b] After 5-h batch hydrogenation of 1-hexene at 25 °C and 1 atm and re-calcination at 500 °C for 2 h.
[c] Based on XRD results.
[d] Based on CO chemisorption results.

Table 2
Results from pulse CO chemisorption and atomic adsorption

Catalyst	CO chemisorption[a] ($\times 10^{18}$molecule CO/g cat.)		Pd dispersion[b] (%)		Pd^0 particle size[c] (nm)		%Pd loading[d] (wt%)	
	Fresh	Spent	Fresh	Spent	Fresh	Spent	Fresh	Spent
Pd/SiO_2-small pore	1.29	0.79	6.5	3.8	17.2	29.2	0.35	0.15
Pd/SiO_2-large pore	1.22	0.61	7.3	4.1	15.3	30.1	0.29	0.18
Pd/MCM-41-small pore	1.20	0.77	4.4	2.3	24.9	45.3	0.41	0.32
Pd/MCM-41-large pore	2.10	1.34	12.0	7.7	9.4	14.7	0.33	0.31

[a] Error of measurement was ± 5%.
[b] Based on the total palladium.
[c] Based on $d = (1.12/D)$ nm [29].
[d] Based on atomic adsorption (AA) results.

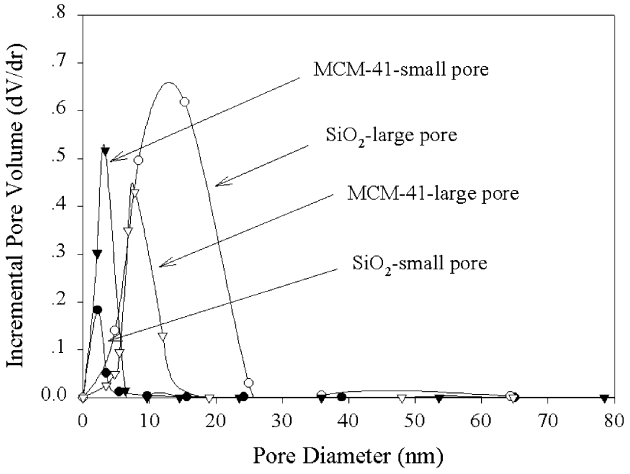

Fig. 1. Pore size distribution of different silica supports.

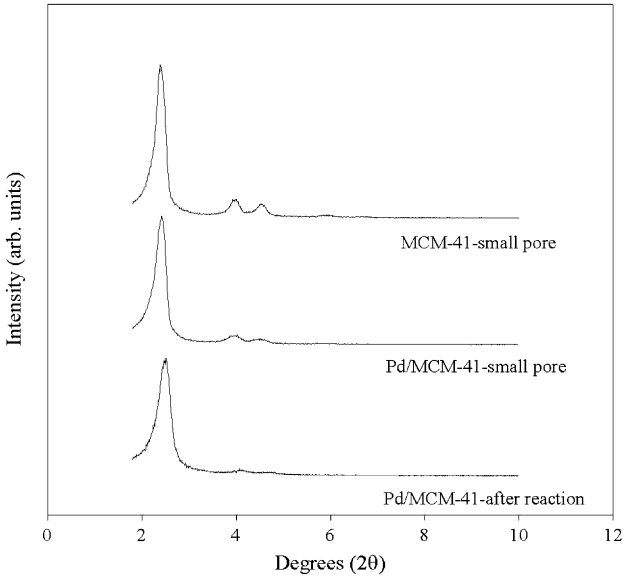

Fig. 2. XRD patterns of MCM-41-small pore and Pd/MCM-41-small pore before and after reaction.

as BET, XRD, TEM, SEM, atomic adsorption, and CO chemisorption. The spent catalysts were collected after one 5-h batch reaction. In order to avoid the influence of carbon deposits on the pore structure and the contrast of SEM and TEM images of the used catalysts. After being taken out from the reactor and dried at room temperature, the catalysts were re-calcined in air at 500 °C for 2 h before characterization to remove any carbon deposits.

The BET surface areas and pore volumes of the original supports and the catalysts before and after reaction are given in Table 1. Except for the low surface area commercial large pore silica, SiO_2-small pore, MCM-41-small pore, and MCM-41-large pore possessed high BET surface areas of 716–921 m^2/g. After impregnation of palladium, the BET surface area and pore volume of the original supports decreased by approximately 6–20%, suggesting that palladium was deposited in some of the pores of the supports. Fig. 1 shows the pore size distribution of the four different silica supports used in this study. A narrow pore size distribution was observed for all the catalyst supports except the commercial large pore silica. The BET surface areas of the spent catalysts ranged between 191 and 546 m^2/g. Since most of the carbon deposits were removed by calcination at 500 °C, the changes in BET surface areas after reaction was probably due to pore blocking by metal sintering and/or destruction of support pore structure after reaction.

The X-ray diffraction patterns of the original MCM-41-small pore and Pd/MCM-41-small pore (before and after reaction) are shown in Fig. 2. The ordered structure of small pore MCM-41 gave XRD peaks at 2.40°, 3.96°, and 4.53° 2θ. After impregnation of palladium the intensities of the XRD peaks for MCM-41 were decreased suggesting either that the structure of MCM-41 became less ordered upon impregnation with Pd or that Pd particles inside the pores caused significant X-ray scattering. In any case, the structure of MCM-41 was not destroyed, although the long-range order of MCM-41 may have shrunk [25]. After reaction, the character-

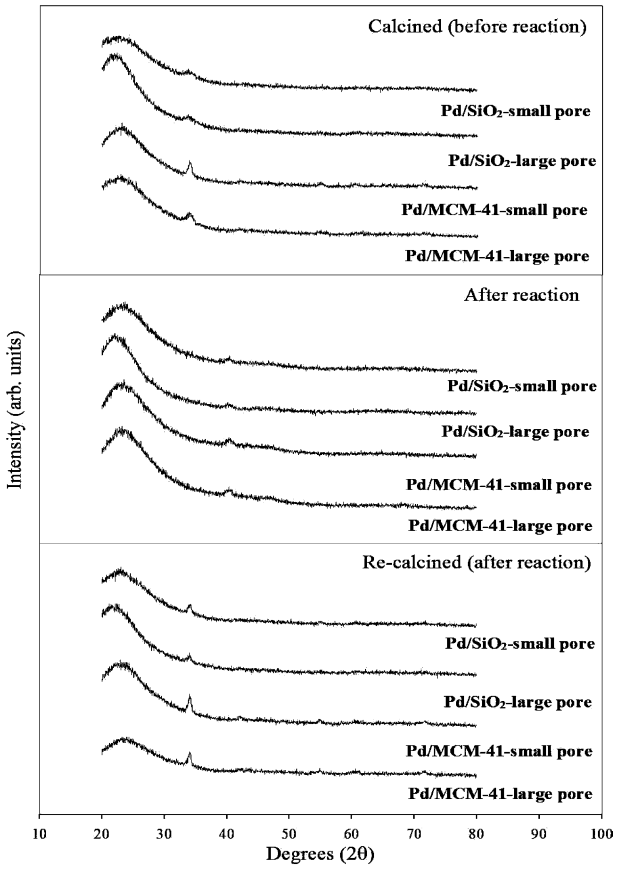

Fig. 3. XRD patterns at high degrees 2θ.

istic peaks of MCM-41-small pore decreased further, probably due to the instability of pure silica MCM-41 and/or the greater X-ray scattering ability of sintered metal particles [26].

The XRD patterns at higher diffraction angles of the different silica supported Pd are shown in Fig. 3. In the calcined state, diffraction peaks for palladium oxide (PdO) were detectable at 33.8° and less so at 42.0°, 54.8°, 60.7°, and 71.4° 2θ. After reaction (before re-calcination), palladium metal (Pd^0) was in evidence with diffraction peaks at 40.1° and less so at 46.6° 2θ. The recovered catalysts were then re-calcined in order to compare the PdO particle sizes before and after reaction. The PdO particle sizes were calculated from XRD line broadening of the peak at 33.8° 2θ using Scherrer's equation [27] and are reported in Table 2. In the calcined catalysts, the PdO particles/clusters were found to be ca. 8–14 nm in the order of Pd/MCM-41-small pore > Pd/SiO_2-large pore > Pd/MCM-41-large pore ≈ Pd/SiO_2-small pore. After reaction and re-calcination, it was found that the PdO particle sizes for all catalyst samples became larger, suggesting sintering of palladium metal particles [28]. Use of large pore supports resulted in the greatest amount of Pd sintering. It should be noted that the lower the surface area, the higher probability of a metal particle to be closed to other ones and therefore the sintering probability is also higher.

Typical TEM micrographs of the fresh and spent supported Pd catalysts are shown in Fig. 4. TEM micrographs were taken in order to physically measure the size of the palladium oxide particles and/or palladium clusters. Since the metal loading is low and the surface area of the sample is very high, in principle it is quite difficult to observe metal dispersion by TEM. However, a

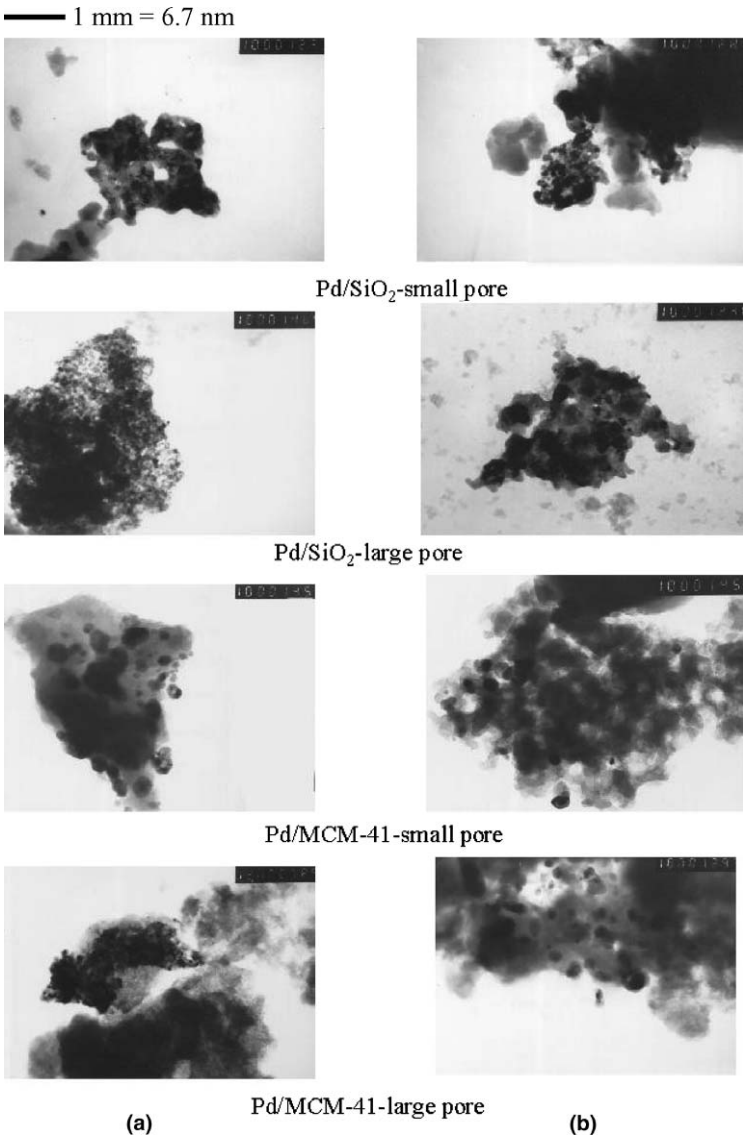

Fig. 4. TEM micrographs of (a) fresh and (b) re-calcined used supported Pd catalysts.

large number of pictures were collected from different portion of the samples in order to obtain further evidence about the dispersion of the palladium. The particle sizes of PdO particles measured from TEM images before and after reaction were found to be in accordance with the results from XRD. The TEM images of the used catalysts were taken after all the carbon deposits have been removed. The differences in PdO particle sizes on different supports then can be ascribed to differences induced by the support on the sintering of Pd during preparation and reaction [9].

Typical SEM micrographs of catalyst particles are shown in Fig. 5. The SEM micrographs show different catalyst particle sizes. For both small pore and large pore MCM-41 supported catalysts, the particle sizes were approximately 20–30 μm, whereas particle sizes of the small and large pore SiO_2 were around 130–150 and 400–500 μm, respectively. It would appear that the size and shape of the catalyst particles were not affected during the 5-h batch liquid-phase hydrogenation reaction suggesting that the different silica supports used in this study have reasonably high attrition resistance.

The amounts of CO chemisorption on the catalysts, the percentages of Pd dispersion, and the Pd metal particle sizes are given in Table 2. The pulse CO chemisorption technique was based on the assumption that one carbon monoxide molecule adsorbs on one palladium site [29–34]. It should be noted that this is an approximation since 1-hexene may not reach all the adsorption sites available for CO adsorption. Before reaction, it was found that Pd/MCM-41-large pore exhibited the highest amount of CO chemisorption, whereas the other cata-

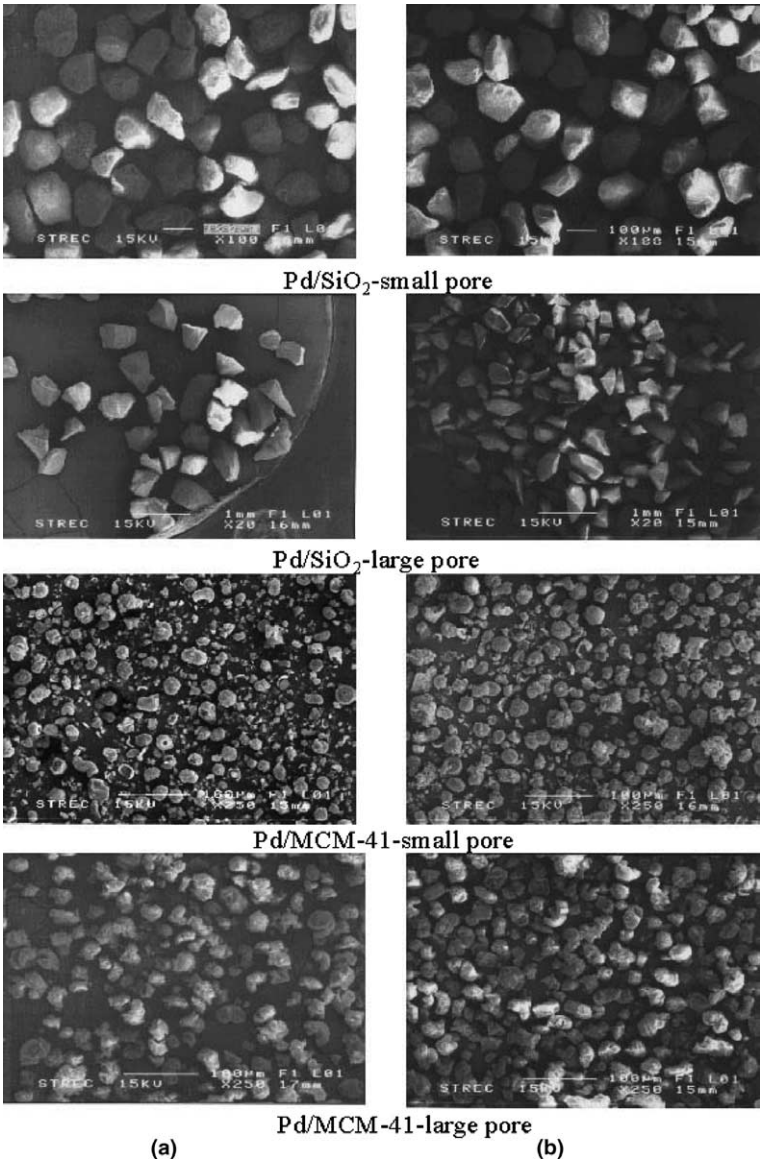

Fig. 5. SEM micrographs of (a) fresh and (b) re-calcined used supported Pd catalysts.

lysts showed similar amounts of CO chemisorption. This was probably due to the dispersion of palladium being better on the large pore MCM-41. The percentages of Pd dispersion before and after reaction were calculated to be in the range of 4.4–12.0% and 2.3–7.7%, respectively, in the descending order of Pd/MCM-41-large pore > Pd/SiO_2-large pore > Pd/SiO_2-small pore > Pd/MCM-41-small pore. Average particle size for reduced Pd^0 was calculated to be in the range of 9.4–24.9 nm before reaction and 14.7–45.3 nm after reaction. These average Pd metal particle sizes calculated based on CO chemisorption are not identical of course to the calculated PdO particle sizes obtained by XRD and TEM. The MCM-41-large pore supported catalysts appeared to have smaller average Pd particle sizes than those on other catalysts, resulting in their relatively high Pd dispersion. After reaction, the amount of CO chemisorption and % Pd dispersion decreased significantly for all catalyst samples by approximately 35–50% of that of the fresh catalysts.

The actual amounts of palladium loading before and after reaction were also determined by atomic adsorption spectroscopy and are given in Table 2. Before reaction, palladium loading on the catalyst samples was approximately 0.29–0.48 wt%. After one 5-h batch hydrogenation reactions of 1-hexene, palladium loading had decreased to 0.15–0.32 wt%. This indicates that leaching of palladium occurred during reaction. The order of the percentages of the amount of palladium leaching was Pd/SiO_2-small pore > Pd/SiO_2-large pore > Pd/MCM-41-small pore $\gg$ Pd/MCM-41-large pore. Pd/MCM-41-large pore showed almost no leaching of palladium into the reaction media within experimental error. The results suggest that the structure of MCM-41 may modify bulk and surface properties of the Pd since Pd metal particles on MCM-41 exhibited different characteristics and catalytic properties compared to those on amorphous silica. An alternative explanation is that Pd/MCM-41-large pore catalyst is likely to have small palladium particles located mostly in the pores of MCM-41, consequently Pd was not prone to leaching compare to the other catalysts. Smaller particles can also interact more with the supports than larger ones. A peculiar metal–support interaction between metal and MCM-41 support has been reported in the literature for CoRu/MCM-41 catalysts, Co was found to interact more with MCM-41 than SiO_2 [35].

4. Conclusions

Type of silica, pore size and pore structure were found to affect characteristics and catalytic properties of the silica supported Pd catalysts in liquid-phase hydrogenation. The catalyst activities were found to be merely dependent on the Pd dispersion, which as itself a function of the support pore structure. There was no evidence for pore diffusion limitations on any of the catalysts since TOFs were nearly identical. Among the four types of the supported Pd catalysts used in this study, Pd/MCM-41-large pore showed the highest Pd dispersion and the highest hydrogenation rate with the lowest amount of metal loss.

Acknowledgements

The financial supports of the Thailand Research Fund (TRF) and TJTTP-JBIC are gratefully acknowledged. The authors also thank Professor Abdel Sayari, University of Ottawa, Canada and Dr. Aticha Chaisuwan, Chulalongkorn University, Thailand for the assistance with MCM-41 preparation.

References

[1] P.N. Rylander, Hydrogenation Methods, Academic Press, New York, 1985.
[2] P. Chou, M.A. Vannice, J. Catal. 107 (1987) 129.
[3] S.D. Jackson, L.A. Shaw, Appl. Catal. A 134 (1996) 91.
[4] V.M. Frolov, O.P. Parengo, A.V. Novikova, L.S. Kovaleva, React. Kinet. Catal. Lett. 25 (1984) 319.
[5] G.M. Cherkashin, L.P. Shuikina, O.P. Parengo, V.M. Frilov, Kinet. Katal. 26 (1985) 1110.
[6] K. Borszeky, T. Mallet, R. Eschiman, W.B. Schweizer, A. Baiker, J. Catal. 161 (1996) 451.
[7] P.L. L'Argentiere, D.A. Liprandi, E.A. Cagnola, N.S. Figoli, Catal. Lett. 44 (1997) 101.
[8] J.P. Mathew, M. Srinivasan, Eur. Polym. J. 31 (1995) 835.
[9] B.M. Choudary, M.L. Kantam, N.M. Reddy, K.K. Rao, Y. Haritha, V. Bhaskar, F. Figueras, A. Tuel, Appl. Catal. A 181 (1999) 139.
[10] W.J. Shen, M. Okumura, Y. Matsumura, M. Haruta, Appl. Catal. A 213 (2001) 225.
[11] F. Pinna, F. Menegazzo, M. Signoretto, P. Canton, G. Fagherazzi, N. Pernicone, Appl. Catal. A 219 (2001) 195.
[12] J.S. Beck, J.C. Vartuli, W.J. Roth, M.E. Leonowicz, C.T. Kresge, K.D. Schmitt, C.T.-W. Chu, D.H. Olson, E.W. Sheppard, S.B. McCullen, J.B. Higgins, J.L. Schlenker, J. Am. Chem. Soc. 114 (1992) 10834.
[13] C.T. Kresge, M.E. Leonowicz, W.J. Roth, J.C. Vartuli, J.S. Beck, Nature 359 (1992) 710.
[14] D. Zhao, J. Feng, Q. Huo, N. Melosh, G.H. Frederickson, B.F. Chmelka, G.C. Stucky, Science 279 (1998) 548.
[15] P.T. Tanev, T.J. Pinnavaia, Science 267 (1995) 865.
[16] A. Corma, A. Martinez, V. Martinez-Soria, J. Catal. 169 (1997) 480.
[17] C. Song, K.M. Reddy, Appl. Catal. A 176 (1999) 1.
[18] S. Shimazu, N. Baba, N. Ichiku, T. Uematsu, J. Mol. Catal. 182 (2002) 343.
[19] D.H. Cho, T.S. Chang, S.K. Ryu, Y.K. Lee, Catal. Lett 64 (2000) 227.
[20] M.K. Dalal, R.N. Ram, Eur. Polym. J. 33 (1997) 1495.
[21] E.A. Sales, M.D. Mendes, F. Bozon-Verduraz, J. Catal. 195 (2000) 96.
[22] Y.Y. Huang, W.M.H. Sachtler, Appl. Catal. A 163 (1997) 245.
[23] R. Takahashi, S. Sato, T. Sodesawa, H. Nishida, Phys. Chem. Chem. Phys. 4 (2002) 3800.

[24] G. van de Lee, V. Ponec, Catal. Rev. Sci. Eng. 29 (1987) 183.
[25] L. Pasqua, F. Testa, R. Aiello, F. Di Renzo, F. Fajula, Micropor. Mesopor. Mater. 44–45 (2001) 111.
[26] B. Marler, U. Oberhagemann, S. Vartmann, H. Gies, Micropor. Mater. 6 (1996) 375.
[27] H.P. Klug, L.E. Alexander, X-ray Diffraction Procedures For Polycrystalline Amorphous Materials, second ed., Wiley, New York, 1974.
[28] O. Dominguez-Quintero, S. Martinez, Y. Henriquez, L. D'Ornelas, H. Krentzien, J. Osuna, J. Mol. Catal. A 197 (2003) 185.
[29] N. Mahata, V. Vishwanathan, J. Catal. 196 (2000) 262.
[30] S.H. Ali, J.G. Goodwin Jr., J. Catal. 176 (1998) 3.
[31] E.A. Sales, G. Bugli, A. Ensuque, M.J. Mendes, F. Bozon-Verduraz, Phys. Chem. Chem. Phys. 1 (1999) 491.
[32] A. Sarkany, Z. Zsoldos, B. Furlong, J.W. Hightower, L. Guczi, J. Catal. 141 (1993) 566.
[33] M.A. Vannice, S.Y. Wang, S.H. Moon, J. Catal. 71 (1981) 152.
[34] N.K. Nag, Catal. Lett. 24 (1994) 37.
[35] J. Panpranot, J.G. Goodwin Jr., A. Sayari, Catal. Today 77 (2002) 269.